

Density Model for Melon-Headed Whale (*Peponocephala electra*) for the U.S. East Coast: Supplementary Report

Model Version 2.1

Duke University Marine Geospatial Ecology Laboratory*

2023-05-27


Citation

When citing our methodology or results generally, please cite Roberts et al. (2016, 2023). The complete references appear at the end of this document. We are preparing a new article for a peer-reviewed journal that will eventually replace those. Until that is published, those are the best general citations.

When citing this model specifically, please use this reference:

Roberts JJ, Yack TM, Cañadas A, Fujioka E, Halpin PN, Barco SG, Boisseau O, Chavez-Rosales S, Cole TVN, Cotter MP, Cummings EW, Davis GE, DiGiovanni Jr. RA, Garrison LP, Gowan TA, Jackson KA, Kenney RD, Khan CB, Lockhart GG, Lomac-MacNair KS, McAlarney RJ, McLellan WA, Mullin KD, Nowacek DP, O'Brien O, Pabst DA, Palka DL, Quintana-Rizzo E, Redfern JV, Rickard ME, White M, Whitt AD, Zoidis AM (2022) Density Model for Melon-Headed Whale (*Peponocephala electra*) for the U.S. East Coast, Version 2.1, 2023-05-27, and Supplementary Report. Marine Geospatial Ecology Laboratory, Duke University, Durham, North Carolina.

Copyright and License

 This document and the accompanying results are © 2023 by the Duke University Marine Geospatial Ecology Laboratory and are licensed under a [Creative Commons Attribution 4.0 International License](https://creativecommons.org/licenses/by/4.0/).

Model Version History

Version	Date	Description
1	2015-01-31	Initial version.
1.1	2015-05-14	Updated calculation of CVs. Switched density rasters to logarithmic breaks. No changes to the model.
1.2	2015-09-26	Updated the documentation. No changes to the model. Model files released as supplementary information to Roberts et al. (2016).

*For questions or to offer feedback please contact Jason Roberts (jason.roberts@duke.edu) and Tina Yack (tina.yack@duke.edu)

(continued)

Version	Date	Description
2	2022-06-20	This model is a major update over the prior version, with substantial additional data, improved statistical methods, and an increased spatial resolution. It was released as part of the final delivery of the U.S. Navy Marine Species Density Database (NMSDD) for the Atlantic Fleet Testing and Training (AFTT) Phase IV Environmental Impact Statement. Several new collaborators joined and contributed survey data: New York State Department of Environmental Conservation, TetraTech, HDR, and Marine Conservation Research. We incorporated additional surveys from all continuing and new collaborators through the end of 2020. (Because some environmental covariates were only available through 2019, certain models only extend through 2019.) We increased the spatial resolution to 5 km and, at NOAA's request, we extended the model further inshore from New York through Maine. We reformulated and refitted all detection functions and spatial models. We updated all environmental covariates to newer products, when available, and added several covariates to the set of candidates. For models that incorporated dynamic covariates, we estimated model uncertainty using a new method that accounts for both model parameter error and temporal variability.
2.1	2023-05-27	Completed the supplementary report documenting the details of this model. Corrected the 5 and 95 percent rasters so that they contain the value 0 where the taxon was assumed absent, rather than NoData. Nothing else was changed.

1 Survey Data

We built this model from data collected between 1998-2020 (Table 1, Figure 1). We excluded surveys that did not target small cetaceans or were otherwise problematic for modeling them. To maintain consistency with the other models developed during the 2022 modeling cycle, most of which excluded data prior to 1998 in order to utilize biological covariates derived from satellite ocean color observations, we also excluded data prior to 1998 from this model. We restricted the model to aerial survey transects with sea states of Beaufort 4 or less (for a few surveys we used Beaufort 3 or less) and shipboard transects with Beaufort 5 or less (for a few we used Beaufort 4 or less). We also excluded transects with poor weather or visibility for surveys that reported those conditions.

Table 1: Survey effort and observations considered for this model. Effort is tallied as the cumulative length of on-effort transects. Observations are the number of groups and individuals encountered while on effort. Off effort observations and those lacking an estimate of group size or distance to the group were excluded.

Institution	Program	Period	Effort	Observations		
			1000s km	Groups	Individuals	Mean Group Size
Aerial Surveys						
HDR	Navy Norfolk Canyon	2018-2019	11	0	0	
NEAq	CNM	2017-2020	2	0	0	
NEAq	MMS-WEA	2017-2020	37	0	0	
NEAq	NLPSC	2011-2015	43	0	0	
NEFSC	AMAPPS	2010-2019	83	0	0	
NEFSC	NARWSS	2003-2016	380	0	0	
NEFSC	Pre-AMAPPS	1999-2008	45	0	0	
NJDEP	NJEBS	2008-2009	9	0	0	
SEFSC	AMAPPS	2010-2020	112	0	0	
SEFSC	MATS	2002-2005	27	0	0	
UNCW	Navy Cape Hatteras	2011-2017	34	1	185	185
UNCW	Navy Jacksonville	2009-2017	92	0	0	
UNCW	Navy Norfolk Canyon	2015-2017	14	0	0	
UNCW	Navy Onslow Bay	2007-2011	49	0	0	
VAMSC	MD DNR WEA	2013-2015	15	0	0	
VAMSC	Navy VACAPES	2016-2017	19	0	0	
VAMSC	VA CZM WEA	2012-2015	21	0	0	
		Total	994	1	185	185
Shipboard Surveys						
MCR	SOTW Visual	2012-2019	8	0	0	
NEFSC	AMAPPS	2011-2016	15	0	0	
NEFSC	Pre-AMAPPS	1998-2007	11	0	0	
SEFSC	AMAPPS	2011-2016	16	0	0	
SEFSC	Pre-AMAPPS	1998-2006	30	2	100	50
		Total	80	2	100	50
		Grand Total	1,075	3	285	95

Table 2: Institutions that contributed surveys used in this model.

Institution	Full Name
HDR	HDR, Inc.
MCR	Marine Conservation Research
NEAq	New England Aquarium
NEFSC	NOAA Northeast Fisheries Science Center
NJDEP	New Jersey Department of Environmental Protection
SEFSC	NOAA Southeast Fisheries Science Center
UNCW	University of North Carolina Wilmington
VAMSC	Virginia Aquarium & Marine Science Center

Table 3: Descriptions and references for survey programs used in this model.

Program	Description	References
AMAPPS	Atlantic Marine Assessment Program for Protected Species	Palka et al. (2017), Palka et al. (2021)
CNM	Northeast Canyons Marine National Monument Aerial Surveys	Redfern et al. (2021)
MATS	Mid-Atlantic Tursiops Surveys	
MD DNR WEA	Aerial Surveys of the Maryland Wind Energy Area	Barco et al. (2015)
MMS-WEA	Marine Mammal Surveys of the MA and RI Wind Energy Areas	Quintana-Rizzo et al. (2021), O'Brien et al. (2022)
NARWSS	North Atlantic Right Whale Sighting Surveys	Cole et al. (2007)
Navy Cape Hatteras	Aerial Surveys of the Navy's Cape Hatteras Study Area	McLellan et al. (2018)
Navy Jacksonville	Aerial Surveys of the Navy's Jacksonville Study Area	Foley et al. (2019)
Navy Norfolk Canyon	Aerial Surveys of the Navy's Norfolk Canyon Study Area	Cotter (2019), McAlarney et al. (2018)
Navy Onslow Bay	Aerial Surveys of the Navy's Onslow Bay Study Area	Read et al. (2014)
Navy VACAPES	Aerial Survey Baseline Monitoring in the Continental Shelf Region of the VACAPES OPAREA	Mallette et al. (2017)
NJEBS	New Jersey Ecological Baseline Study	Geo-Marine, Inc. (2010), Whitt et al. (2015)
NLPSC	Northeast Large Pelagic Survey Collaborative Aerial Surveys	Leiter et al. (2017), Stone et al. (2017)
Pre-AMAPPS	Pre-AMAPPS Marine Mammal Abundance Surveys	Mullin and Fulling (2003), Garrison et al. (2010), Palka (2006)
SOTW Visual	R/V Song of the Whale Visual Surveys	Ryan et al. (2013)
VA CZM WEA	Virginia CZM Wind Energy Area Surveys	Mallette et al. (2014), Mallette et al. (2015)

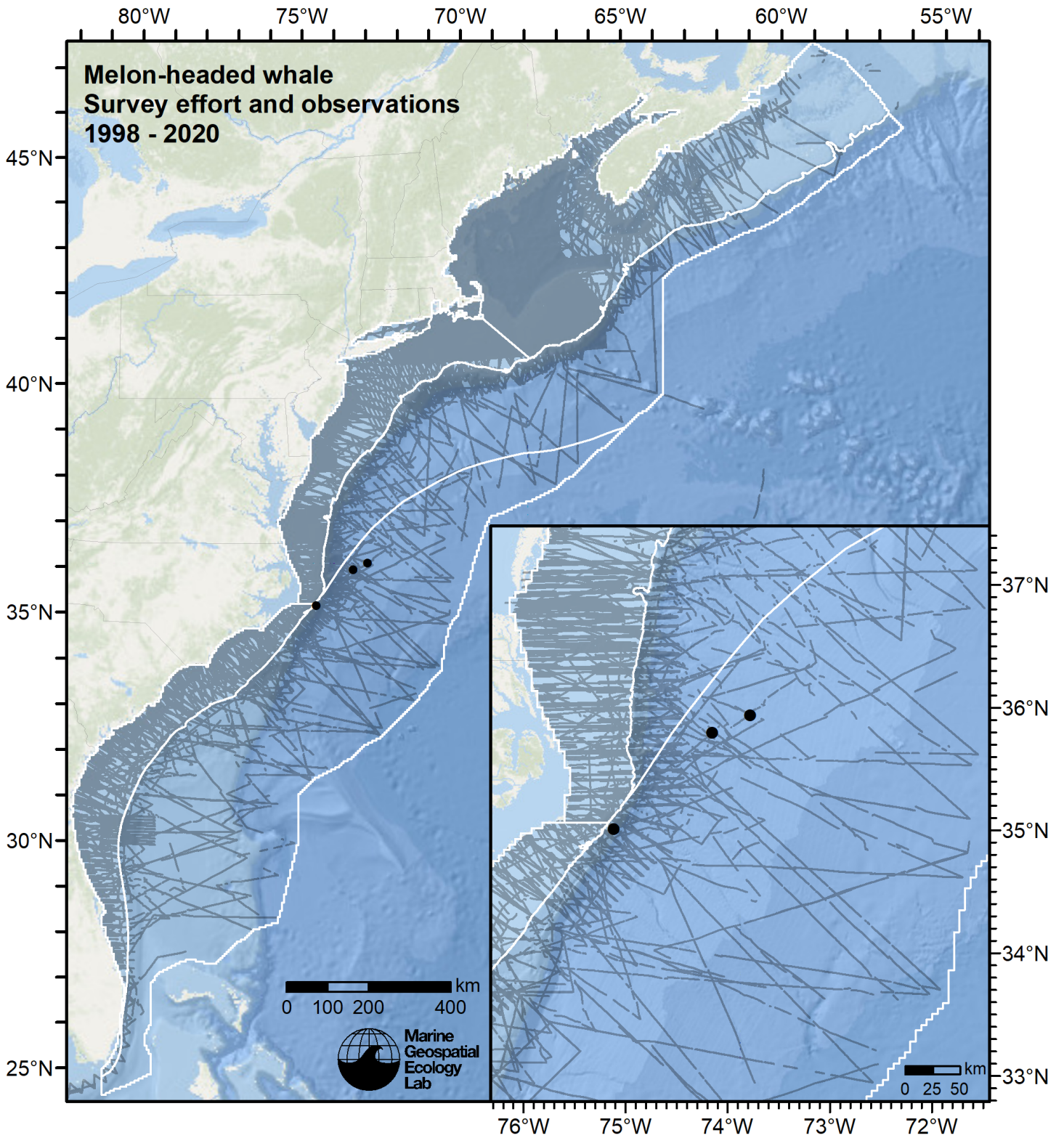


Figure 1: Survey effort and melon-headed whale observations available for density modeling, after detection functions were applied, and excluded segments and truncated observations were removed. White outlines show the strata for which density estimates were derived.

2 Classification of Ambiguous Sightings

Observers occasionally experience difficulty identifying species, due to poor sighting conditions or phenotypic similarities between the possible choices. For example, observers may not always be able to distinguish fin whales from sei whales due their similar size and shape. When this happens, observers will report an ambiguous identification, such as “fin or sei whale”. In our density models, we handled ambiguous identifications in three ways:

1. For sightings with very generic identifications such as “large whale”, we discarded the sightings. These sightings represented a clear minority when compared to those with definitive species identifications, but they are uncounted animals and our density models may therefore underestimate density to some degree.
2. For sightings of certain taxa in which a large majority of identifications were ambiguous (e.g. “unidentified pilot whale”) rather than specific (e.g. “short-finned pilot whale” or “long-finned pilot whale”), it was not tractable to model the individual species so we modeled the generic taxon instead.
3. For sightings that reported an ambiguous identification of two species (e.g. “fin or sei whale”) that are known to exhibit different habitat preferences or typically occur in different group sizes, and for which we had sufficient number of definitive sightings of both species, we first fitted a predictive model that classified the ambiguous sightings into one species or the other and then included the resulting classified sightings in the density models for each of the two species.

This section describes how we classified the third category of ambiguous sightings reported as “pygmy killer or melon-headed whale” into one species or the other.

For the predictive model, we used the cforest classifier (Hothorn et al. 2006), an elaboration of the classic random forest classifier (Breiman 2001). First, we trained a binary classifier using the sightings that reported definitive species identifications (“pygmy killer whale” and “melon-headed whale”). To increase the range of sampling of the classification model’s covariates, the training data may have included additional surveys not considered for the density model, as well as transects from outside the spatial and temporal extents of the density model. Only on-effort sightings were used. We used the species ID as the response variable and the sighting group size as the covariate.

We used receiver operating characteristic (ROC) curve analysis to select a threshold for classifying the probabilistic predictions of species identifications made by the model into a binary result of one species or another. For the classification threshold, we selected the value that maximized the Youden index (Perkins and Schisterman 2006). Then, for all sightings reporting the ambiguous identification, we classified each as either one species or the other by processing the covariate values observed for it through the fitted model. We then included the classified sightings in the detection functions and density models. The sightings reported elsewhere in this document incorporate both the definitive sightings and the classified sightings, unless otherwise noted.

2.1 Classification Model

MODEL SUMMARY:

=====

Random Forest using Conditional Inference Trees

Number of trees: 1000

Response: factor(OriginalScientificName)

Input: GroupSize

Number of observations: 55

Number of variables tried at each split: 5

Estimated predictor variable importance (conditional = FALSE):

Importance

GroupSize 0.412

MODEL PERFORMANCE SUMMARY:

=====

Statistics calculated from the training data.

Area under the ROC curve (auc) = 0.998
Mean cross-entropy (mxe) = 0.058
Precision-recall break-even point (prbe) = -0.000
Root-mean square error (rmse) = 0.125

User-specified cutoff = 0.500

Confusion matrix for that cutoff:

	Actual <i>Peponocephala electra</i>	Actual <i>Feresa attenuata</i>	Total
Predicted <i>Peponocephala electra</i>	35	1	36
Predicted <i>Feresa attenuata</i>	0	19	19
Total	35	20	55

Model performance statistics for that cutoff:

Accuracy (acc) = 0.982
Error rate (err) = 0.018
Rate of positive predictions (rpp) = 0.655
Rate of negative predictions (rnp) = 0.345

True positive rate (tpr, or sensitivity) = 1.000
False positive rate (fpr, or fallout) = 0.050
True negative rate (tnr, or specificity) = 0.950
False negative rate (fnr, or miss) = 0.000

Positive prediction value (ppv, or precision) = 0.972
Negative prediction value (npv) = 1.000
Prediction-conditioned fallout (pcfall) = 0.028
Prediction-conditioned miss (pcmiss) = 0.000

Matthews correlation coefficient (mcc) = 0.961
Odds ratio (odds) = Inf
SAR = 0.701

Cohen's kappa (K) = 0.960

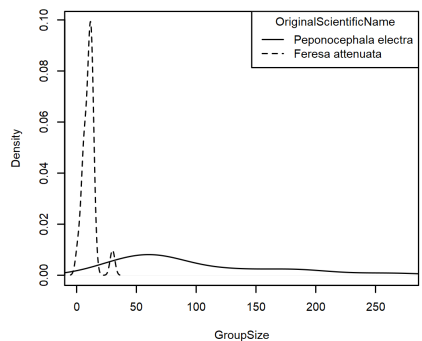


Figure 2: Density histogram showing the per-species distribution of of the GroupSize covariate in the ambiguous sighting classification model.

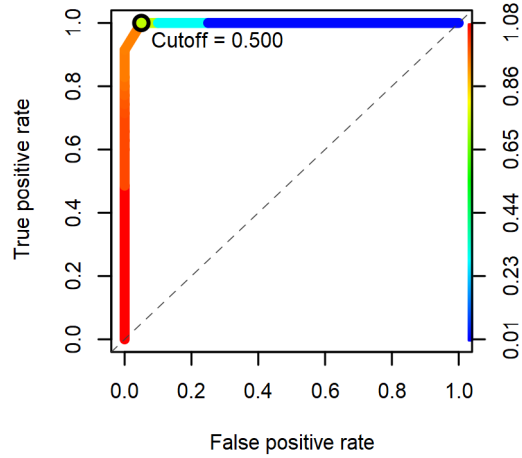


Figure 3: Receiver operating characteristic (ROC) curve summarizing the predictive performance of the ambiguous sighting classification model.

2.2 Classifications Performed

Table 4: Summary of the definitive sightings used to train the classification model, the ambiguous sightings to which the model was applied, and their resulting classifications. To increase the range of sampling of the classification model’s covariates, the training data may have included additional surveys not considered for the density model, as well as transects from outside the spatial and temporal extents of the density model. Only on-effort sightings were used.

Institution	Program	Definitive		Ambiguous	Classified	
		F. attenuata	P. electra		F. attenuata	P. electra
Aerial Surveys						
SEFSC	GulfCet I	0	0	8	3	5
SEFSC	GulfCet II	3	0	0	0	0
U. La Rochelle	REMMOA	0	1	3	3	0
UNCW	Navy Cape Hatteras	0	2	0	0	0
	Total	3	3	11	6	5
Shipboard Surveys						
NEFSC	AMAPPS	1	0	0	0	0
SEFSC	AMAPPS	0	0	2	2	0
SEFSC	GOM Oceanic CetShip	8	18	4	2	2
SEFSC	GOM Shelf CetShip	0	1	0	0	0
SEFSC	GoMMAPPS	1	4	2	2	0
SEFSC	Pre-AMAPPS	0	2	4	4	0
SEFSC	Pre-GoMMAPPS	7	6	1	1	0
SEFSC	SEFSC Caribbean	0	1	1	0	1
	Total	17	32	14	11	3
Grand Total		20	35	25	17	8

3 Detection Functions

3.1 Without a Taxonomic Covariate

We fitted the detection functions in this section to pools of species with similar detectability characteristics but could not use a taxonomic identification as a covariate to account for differences between them. We usually took this approach after trying the taxonomic covariate and finding it had insufficient statistical power to be retained. We also resorted to it when the focal taxon being modeled had too few observations to be allocated its own taxonomic covariate level and was too poorly known for us to confidently determine which other taxa we could group it with.

3.1.1 Aerial Surveys

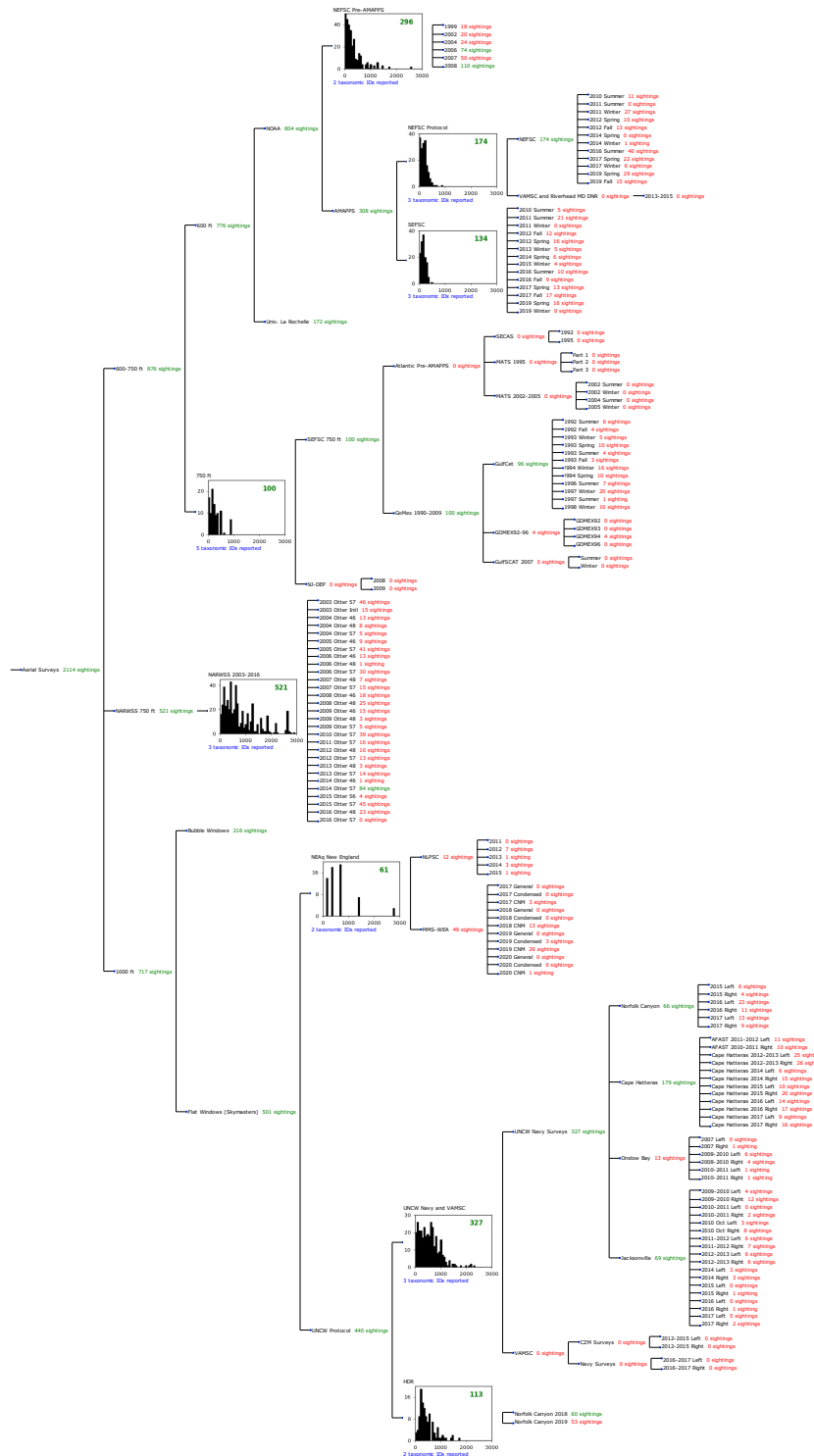


Figure 4: Detection hierarchy for aerial surveys, showing how they were pooled during detectability modeling, for detection functions that pooled multiple taxa but could not use a taxonomic covariate to account for differences between them. Each histogram represents a detection function and summarizes the perpendicular distances of observations that were pooled to fit it, prior to truncation. Observation counts, also prior to truncation, are shown in green when they met the recommendation of Buckland et al. (2001) that detection functions utilize at least 60 sightings, and red otherwise. For rare taxa, it was not always possible to meet this recommendation, yielding higher statistical uncertainty. During the spatial modeling stage of the analysis, effective strip widths were computed for each survey using the closest detection function above it in the hierarchy (i.e. moving from right to left in the figure). Surveys that do not have a detection function above them in this figure were either addressed by a detection function presented in a different section of this report, or were omitted from the analysis.

3.1.1.1 NEFSC Pre-AMAPPS

After right-truncating observations greater than 1300 m, we fitted the detection function to the 289 observations that remained (Table 5). The selected detection function (Figure 5) used a hazard rate key function with no covariates.

Table 5: Observations used to fit the NEFSC Pre-AMAPPS detection function.

ScientificName	n
Globicephala	148
Grampus griseus	141
Total	289

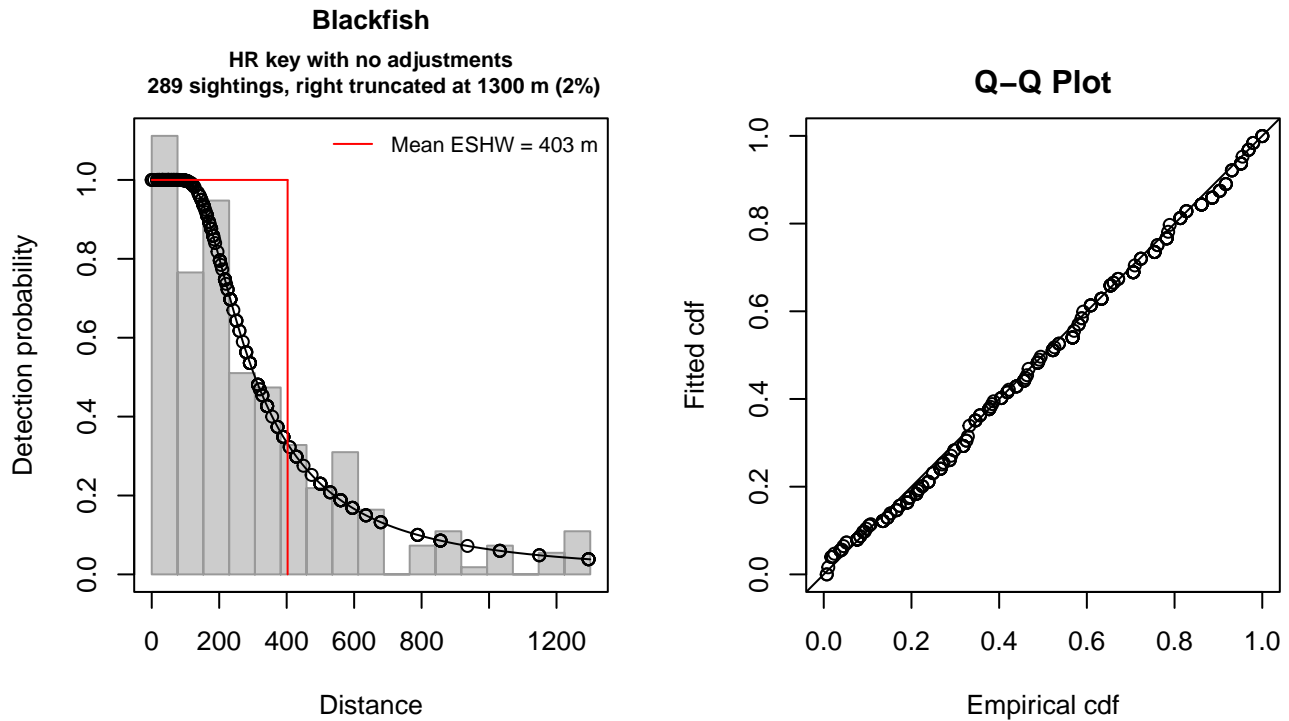


Figure 5: NEFSC Pre-AMAPPS detection function and Q-Q plot showing its goodness of fit.

Statistical output for this detection function:

```
Summary for ds object
Number of observations : 289
Distance range       : 0 - 1300
AIC                  : 3863.885
```

```
Detection function:
Hazard-rate key function
```

```
Detection function parameters
Scale coefficient(s):
      estimate      se
(Intercept) 5.540493 0.1221542
```

```
Shape coefficient(s):
      estimate      se
(Intercept) 0.6890237 0.1060228
```

	Estimate	SE	CV
Average p	0.3098149	0.02386401	0.07702667
N in covered region	932.8151840	85.09243937	0.09122111

Distance sampling Cramer-von Mises test (unweighted)
 Test statistic = 0.049395 p = 0.879943

3.1.1.2 NEFSC AMAPPS Protocol

After right-truncating observations greater than 400 m, we fitted the detection function to the 164 observations that remained (Table 6). The selected detection function (Figure 6) used a hazard rate key function with Beaufort (Figure 7) as a covariate.

Table 6: Observations used to fit the NEFSC AMAPPS Protocol detection function.

ScientificName	n
Globicephala	76
Grampus griseus	87
Orcinus orca	1
Total	164

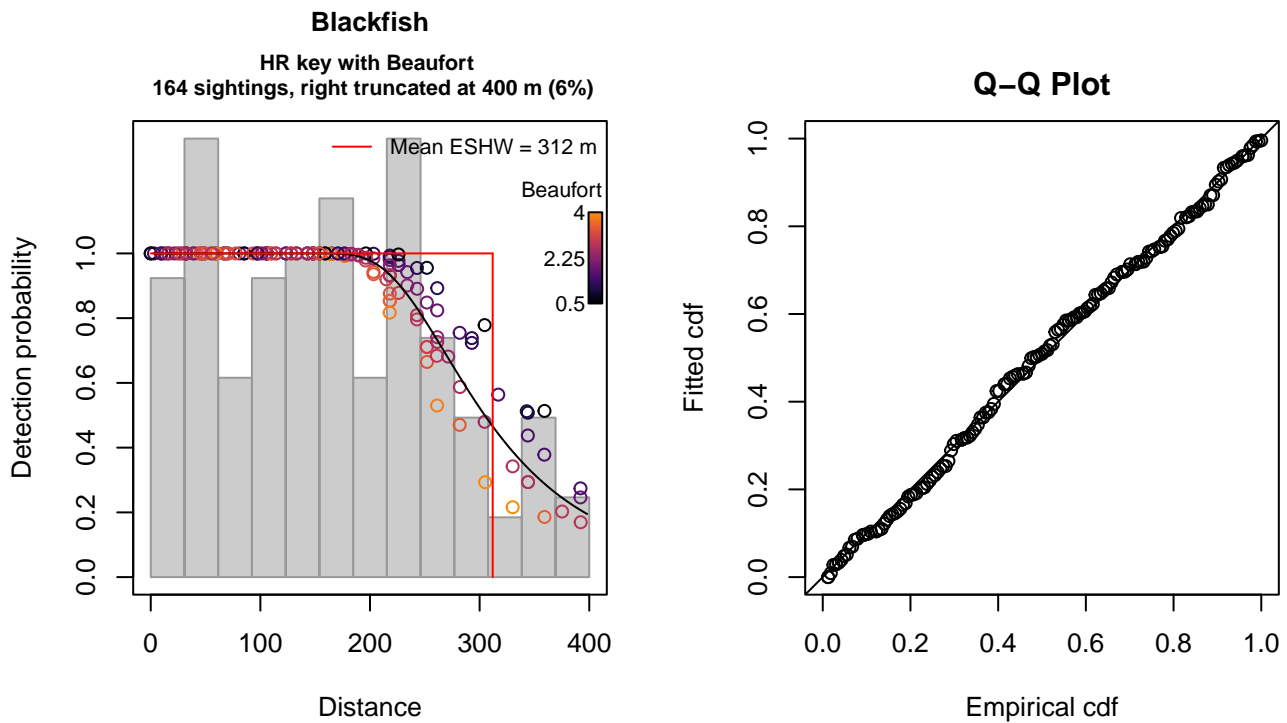


Figure 6: NEFSC AMAPPS Protocol detection function and Q-Q plot showing its goodness of fit.

Statistical output for this detection function:

```
Summary for ds object
Number of observations : 164
Distance range       : 0 - 400
AIC                  : 1943.903
```

```
Detection function:
Hazard-rate key function
```

```
Detection function parameters
```


Scale coefficient(s):
 estimate se
(Intercept) 5.85716562 0.18022637
Beaufort -0.09331802 0.07079169

Shape coefficient(s):
 estimate se
(Intercept) 1.49927 0.3557806

	Estimate	SE	CV
Average p	0.7768428	0.04359073	0.05611268
N in covered region	211.1109209	14.20480094	0.06728596

Distance sampling Cramer-von Mises test (unweighted)
Test statistic = 0.038316 p = 0.941631

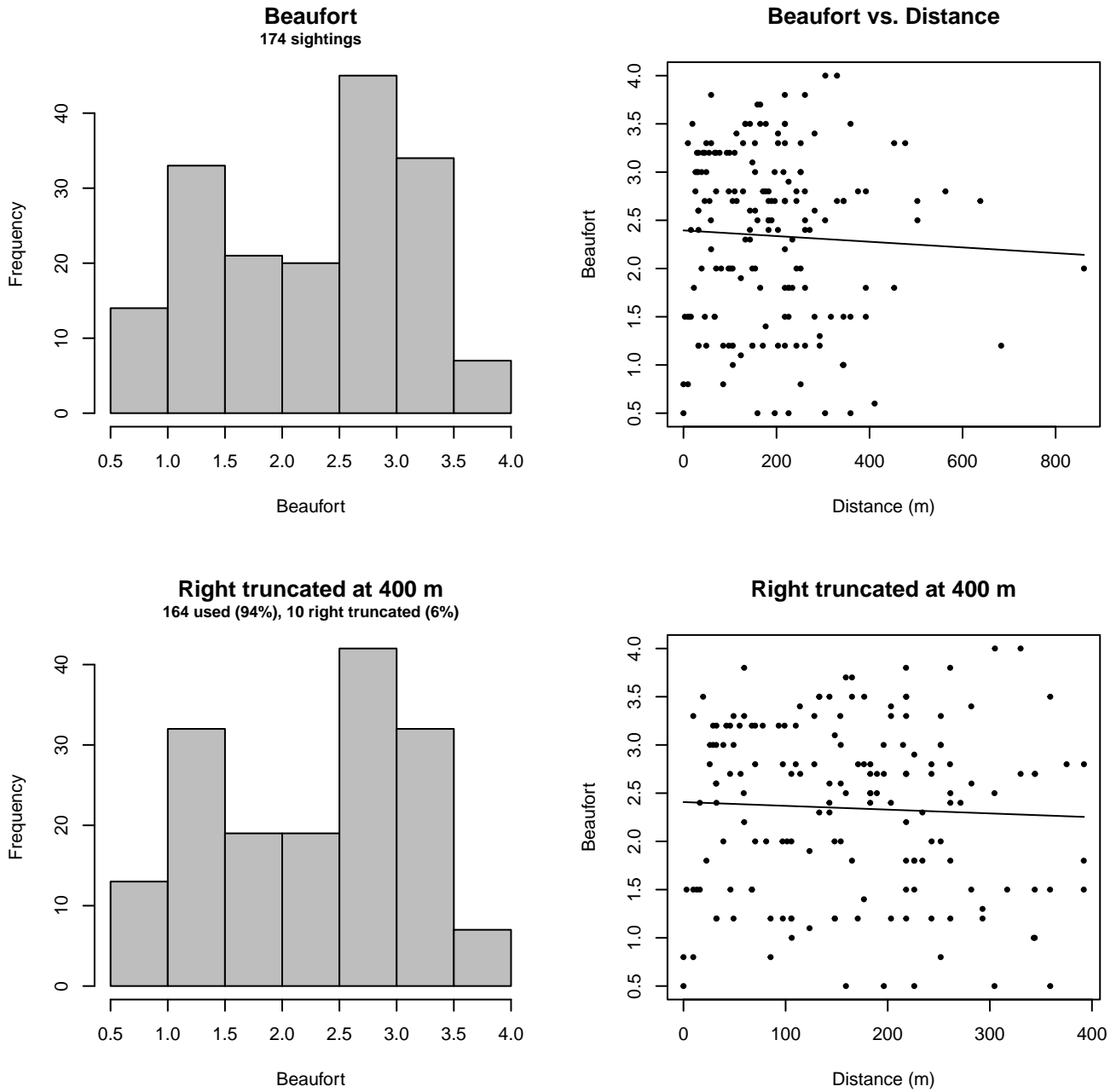


Figure 7: Distribution of the Beaufort covariate before (top row) and after (bottom row) observations were truncated to fit the NEFSC AMAPPS Protocol detection function.

3.1.1.3 SEFSC AMAPPS

After right-truncating observations greater than 400 m and left-truncating observations less than 50 m (Figure 9), we fitted the detection function to the 119 observations that remained (Table 7). The selected detection function (Figure 8) used a hazard rate key function with Beaufort (Figure 10) as a covariate.

Table 7: Observations used to fit the SEFSC AMAPPS detection function.

ScientificName	n
Globicephala	66
Grampus griseus	53
Total	119

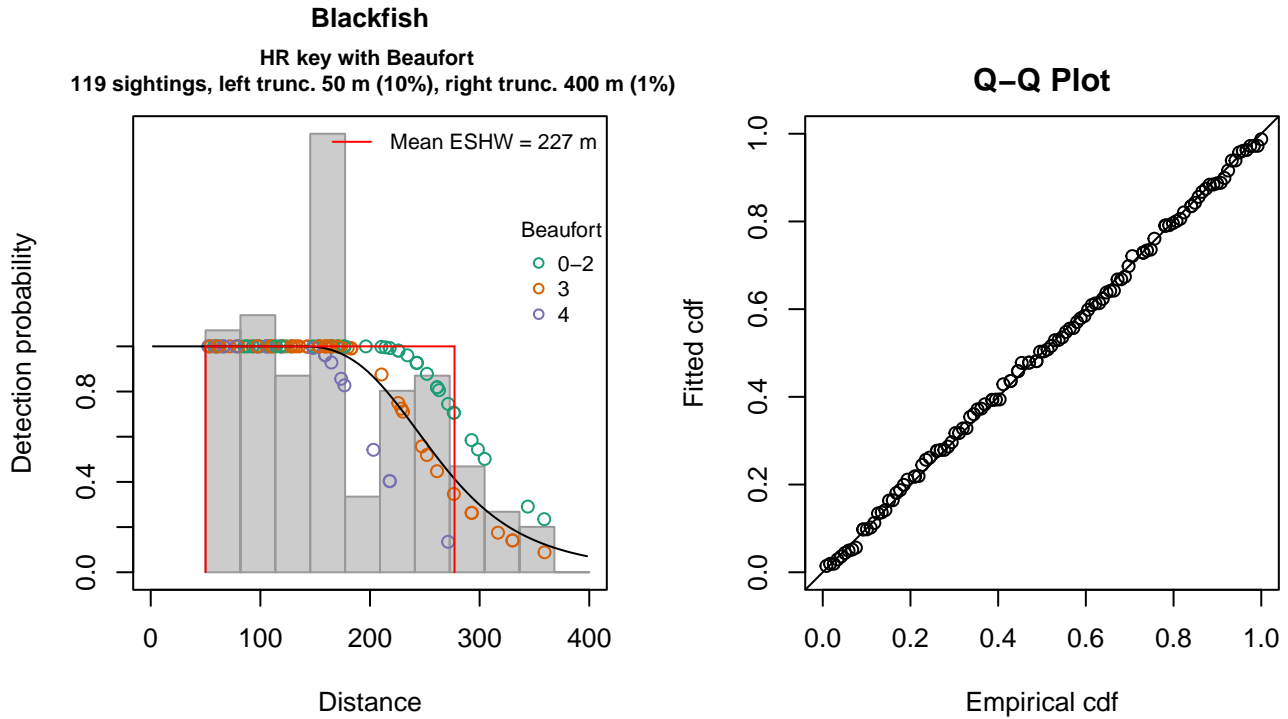


Figure 8: SEFSC AMAPPS detection function and Q-Q plot showing its goodness of fit.

Statistical output for this detection function:

Summary for ds object

Number of observations : 119
 Distance range : 50 - 400
 AIC : 1349.888

Detection function:

Hazard-rate key function

Detection function parameters

Scale coefficient(s):

	estimate	se
(Intercept)	5.6569520	0.1026861
Beaufort3	-0.1814855	0.1309136
Beaufort4	-0.3857171	0.1640754

Shape coefficient(s):

	estimate	se
(Intercept)	1.761805	0.3262538

	Estimate	SE	CV
Average p	0.6336189	0.04206604	0.06639012
N in covered region	187.8100597	16.38859266	0.08726153

Distance sampling Cramer-von Mises test (unweighted)

Test statistic = 0.019109 p = 0.997756

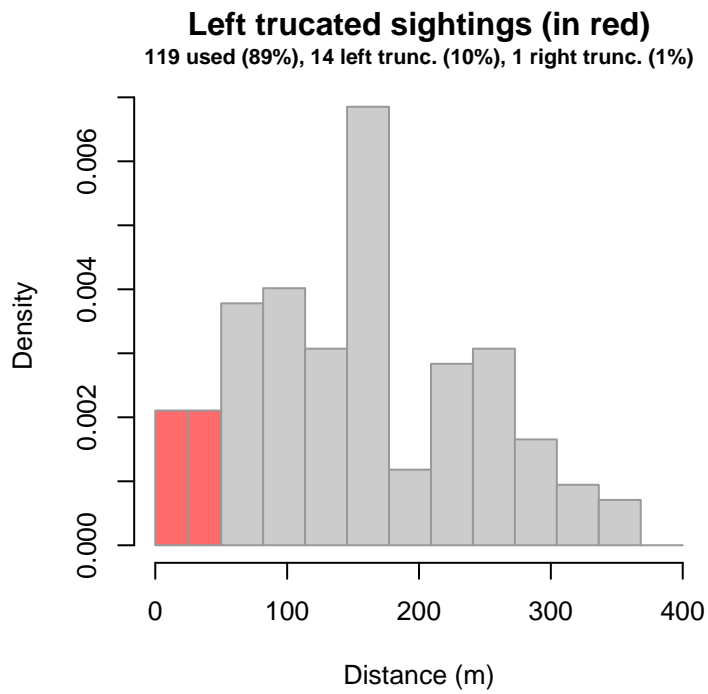


Figure 9: Density histogram of observations used to fit the SEFSC AMAPPS detection function, with the left-most bar showing observations at distances less than 50 m, which were left-truncated and excluded from the analysis [Buckland et al. (2001)]. (This bar may be very short if there were very few left-truncated sightings, or very narrow if the left truncation distance was very small; in either case it may not appear red.)

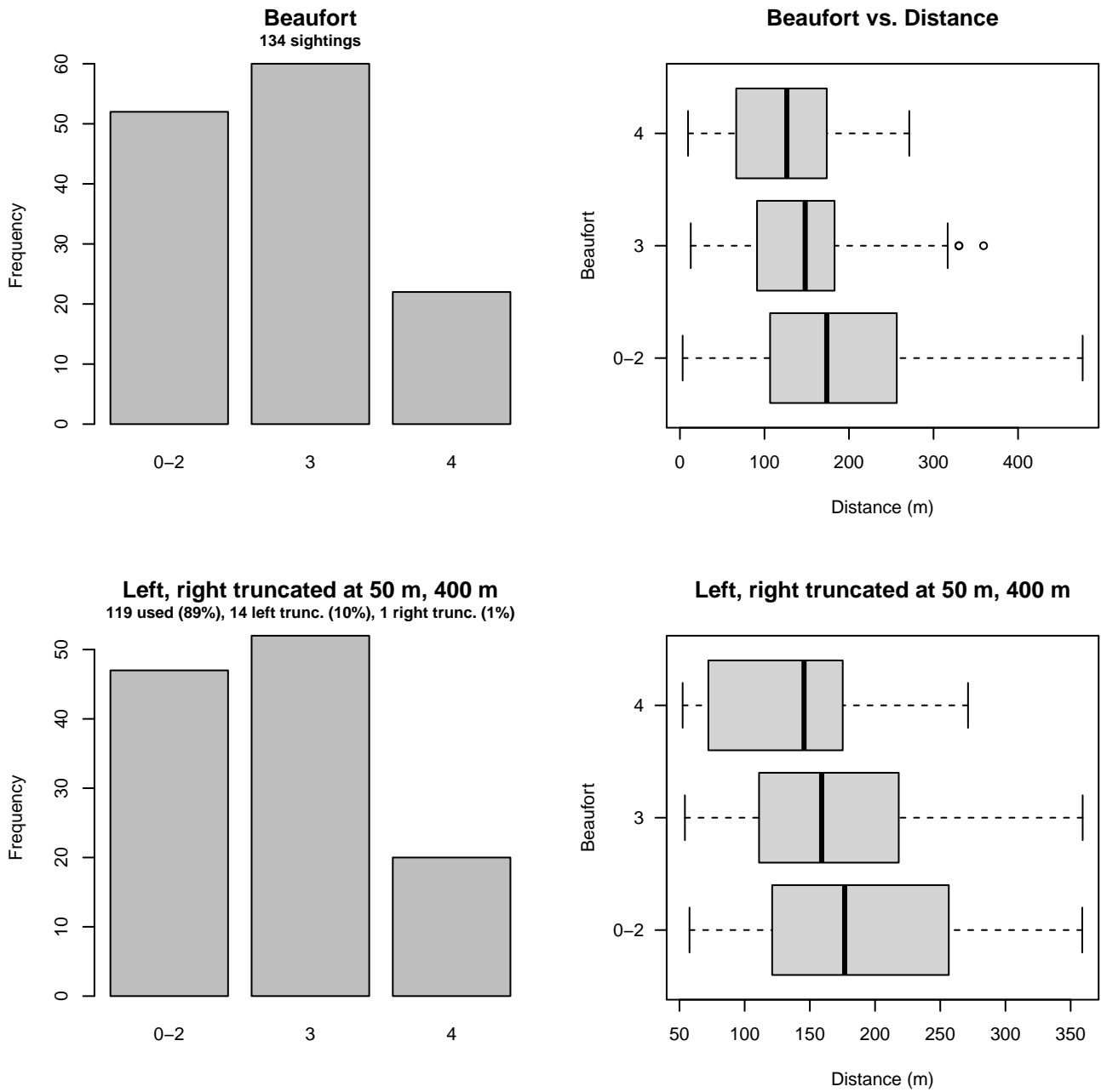


Figure 10: Distribution of the Beaufort covariate before (top row) and after (bottom row) observations were truncated to fit the SEFSC AMAPPS detection function.

3.1.1.4 750 ft

After right-truncating observations greater than 629 m, we fitted the detection function to the 93 observations that remained (Table 8). The selected detection function (Figure 11) used a hazard rate key function with no covariates.

Table 8: Observations used to fit the 750 ft detection function.

ScientificName	n
Feresa attenuata	3
Feresa attenuata/Peponocephala electra	7
Globicephala	12
Grampus griseus	69
Pseudorca crassidens	2
Total	93

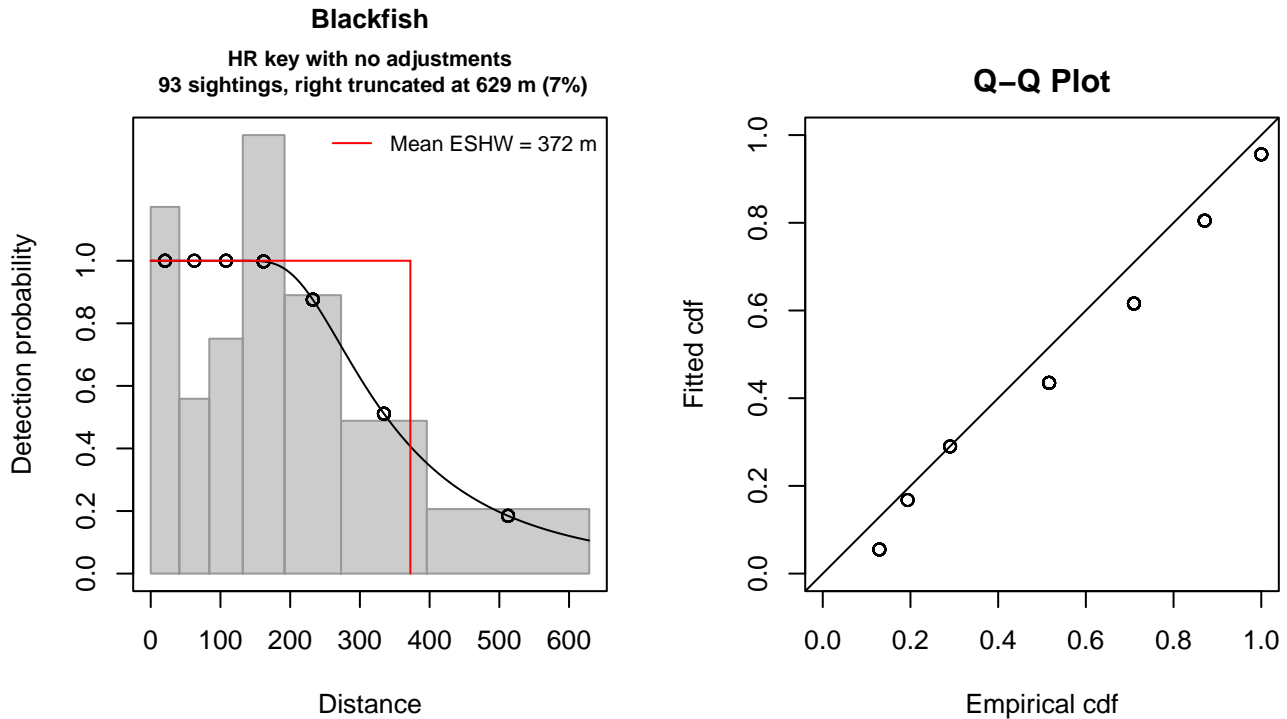


Figure 11: 750 ft detection function and Q-Q plot showing its goodness of fit.

Statistical output for this detection function:

Summary for ds object

Number of observations : 93
 Distance range : 0 - 629
 AIC : 359.4726

Detection function:

Hazard-rate key function

Detection function parameters

Scale coefficient(s):
 estimate se
 (Intercept) 5.698811 0.1702564

Shape coefficient(s):
 estimate se
 (Intercept) 1.07856 0.3654486

	Estimate	SE	CV
Average p	0.5920954	0.06138719	0.1036779

N in covered region 157.0692704 19.32345801 0.1230251

Distance sampling Cramer-von Mises test (unweighted)

Test statistic = 0.271977 p = 0.162483

3.1.1.5 NARWSS 2003-2016

After right-truncating observations greater than 2905 m, we fitted the detection function to the 485 observations that remained (Table 9). The selected detection function (Figure 12) used a hazard rate key function with Beaufort (Figure 13) as a covariate.

Table 9: Observations used to fit the NARWSS 2003-2016 detection function.

ScientificName	n
Globicephala	376
Grampus griseus	106
Orcinus orca	3
Total	485

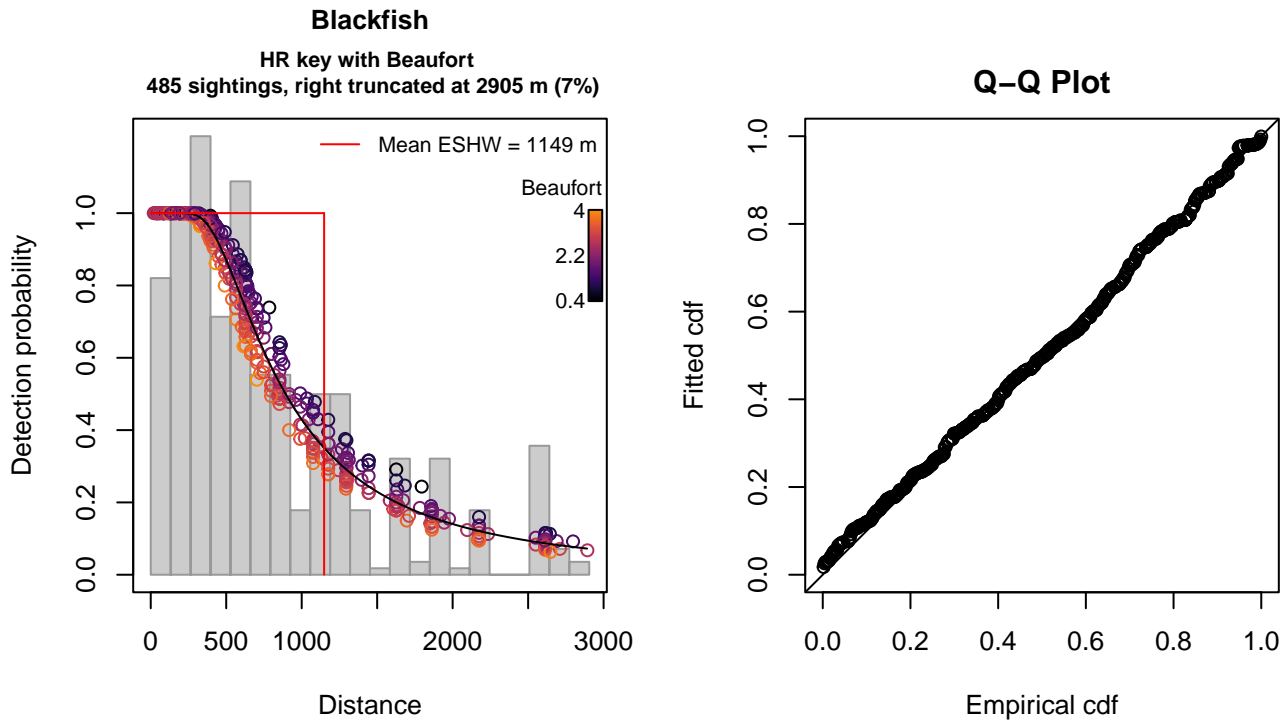


Figure 12: NARWSS 2003-2016 detection function and Q-Q plot showing its goodness of fit.

Statistical output for this detection function:

Summary for ds object

Number of observations : 485
Distance range : 0 - 2905
AIC : 7420.46

Detection function:

Hazard-rate key function

Detection function parameters

Scale coefficient(s):

	estimate	se
(Intercept)	6.8787415	0.22789350
Beaufort	-0.1141738	0.08537414

Shape coefficient(s):

	estimate	se
(Intercept)	0.6421837	0.09908371

	Estimate	SE	CV
Average p	0.393189	0.02454407	0.06242307
N in covered region	1233.503530	88.54090900	0.07178002

Distance sampling Cramer-von Mises test (unweighted)

Test statistic = 0.097833 p = 0.595605

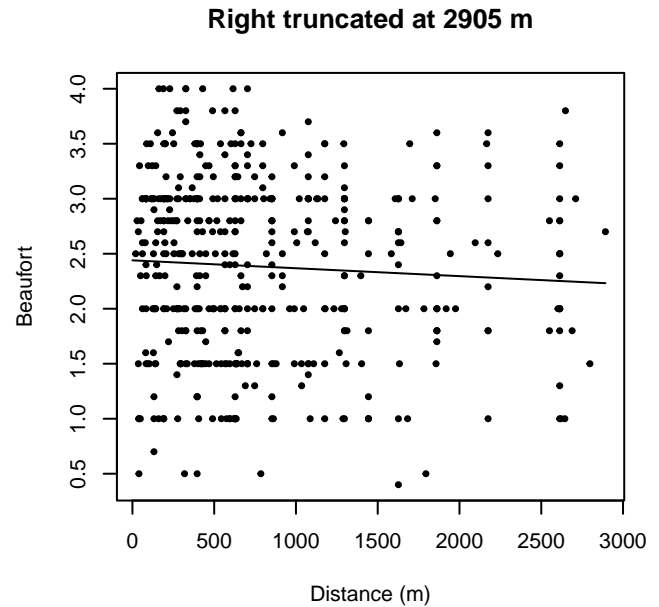
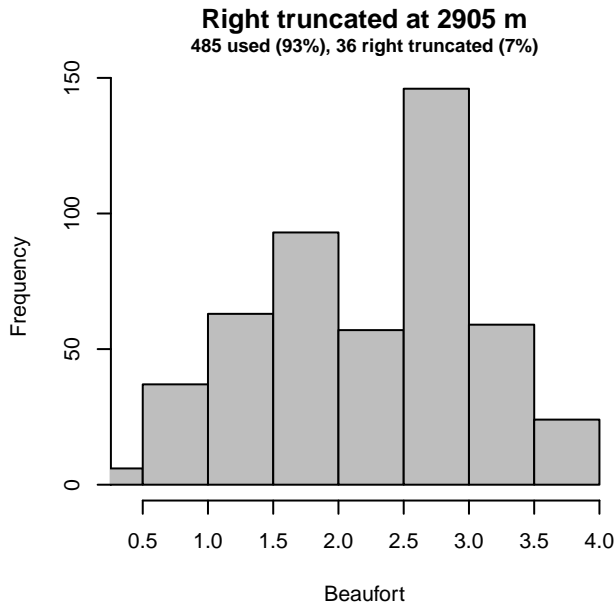
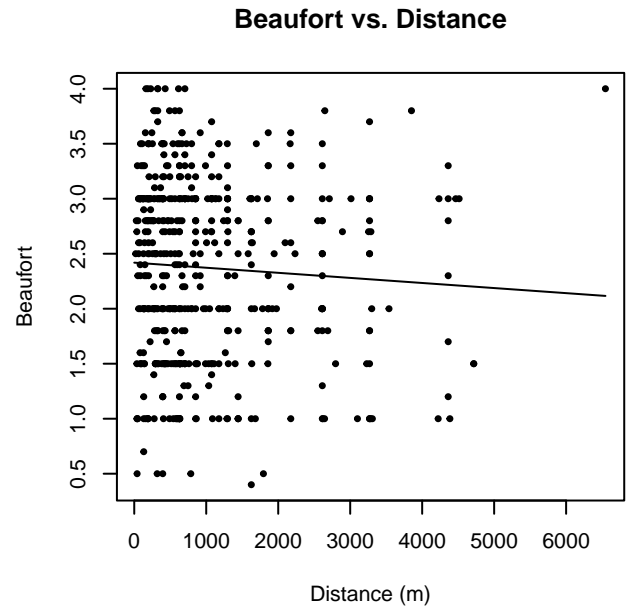
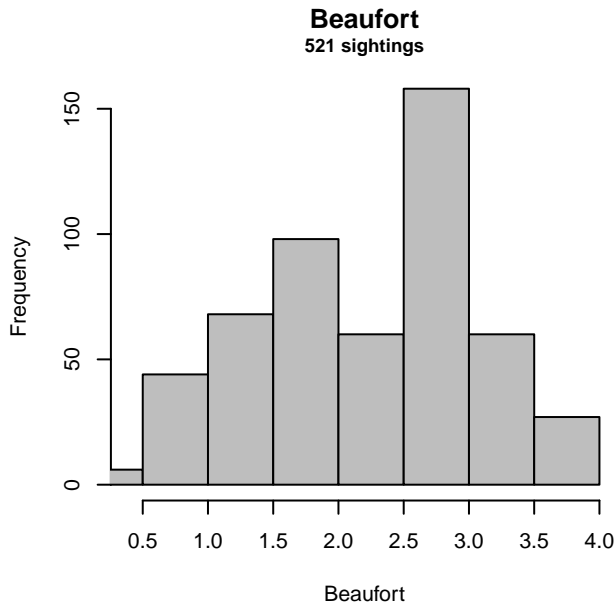


Figure 13: Distribution of the Beaufort covariate before (top row) and after (bottom row) observations were truncated to fit the NARWSS 2003-2016 detection function.

3.1.1.6 NEAq New England

After right-truncating observations greater than 1852 m and left-truncating observations less than 71 m (Figure 15), we fitted the detection function to the 58 observations that remained (Table 10). The selected detection function (Figure 14) used a half normal key function with no covariates.

Table 10: Observations used to fit the NEAq New England detection function.

ScientificName	n
Globicephala	16
Grampus griseus	42
Total	58

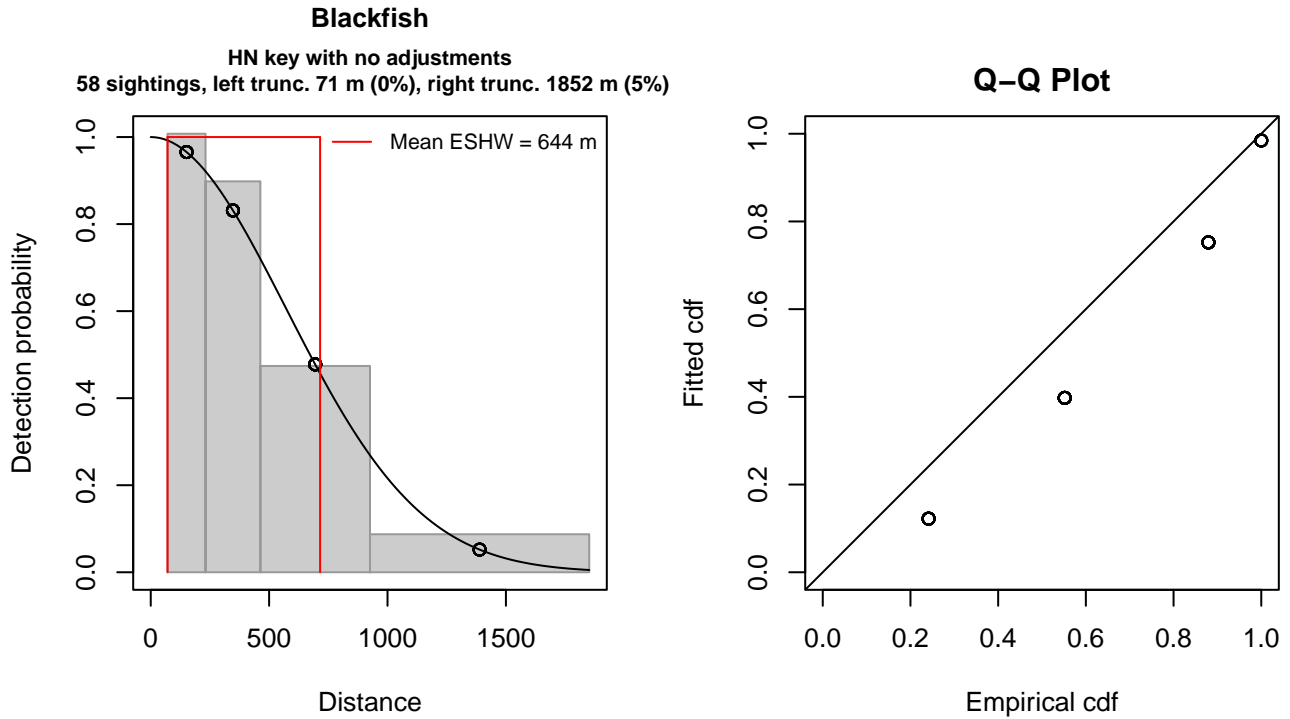


Figure 14: NEAq New England detection function and Q-Q plot showing its goodness of fit.

Statistical output for this detection function:

Summary for ds object

Number of observations : 58
 Distance range : 71 - 1852
 AIC : 156.0466

Detection function:

Half-normal key function

Detection function parameters

Scale coefficient(s):

	estimate	se
(Intercept)	6.347853	0.1032999

	Estimate	SE	CV
Average p	0.3617668	0.04089634	0.1130461
N in covered region	160.3242530	24.72501947	0.1542188

Distance sampling Cramer-von Mises test (unweighted)

Test statistic = 0.430759 p = 0.060002

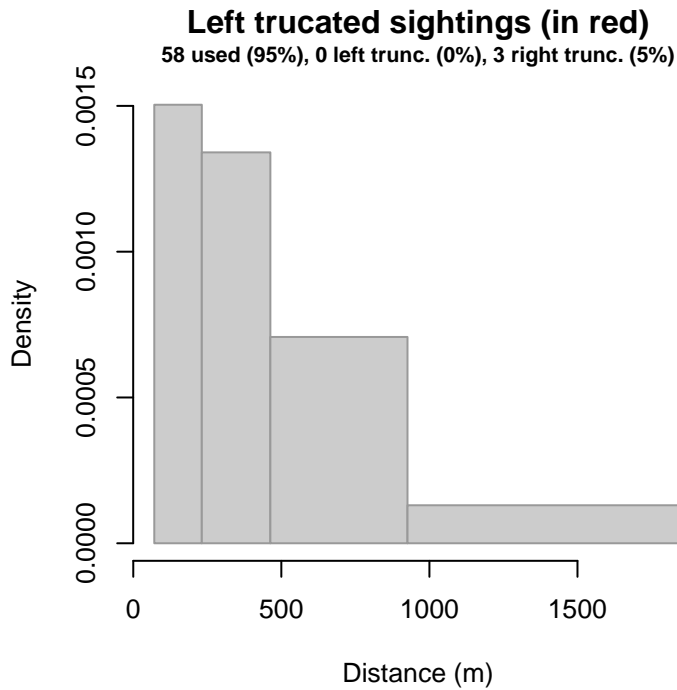


Figure 15: Density histogram of observations used to fit the NEAq New England detection function, with the left-most bar showing observations at distances less than 71 m, which were left-truncated and excluded from the analysis [Buckland et al. (2001)]. (This bar may be very short if there were very few left-truncated sightings, or very narrow if the left truncation distance was very small; in either case it may not appear red.)

3.1.1.7 UNCW Navy and VAMSC

After right-truncating observations greater than 1300 m, we fitted the detection function to the 312 observations that remained (Table 11). The selected detection function (Figure 16) used a hazard rate key function with Visibility (Figure 17) as a covariate.

Table 11: Observations used to fit the UNCW Navy and VAMSC detection function.

ScientificName	n
Globicephala macrorhynchus	223
Grampus griseus	88
Peponocephala electra	1
Total	312

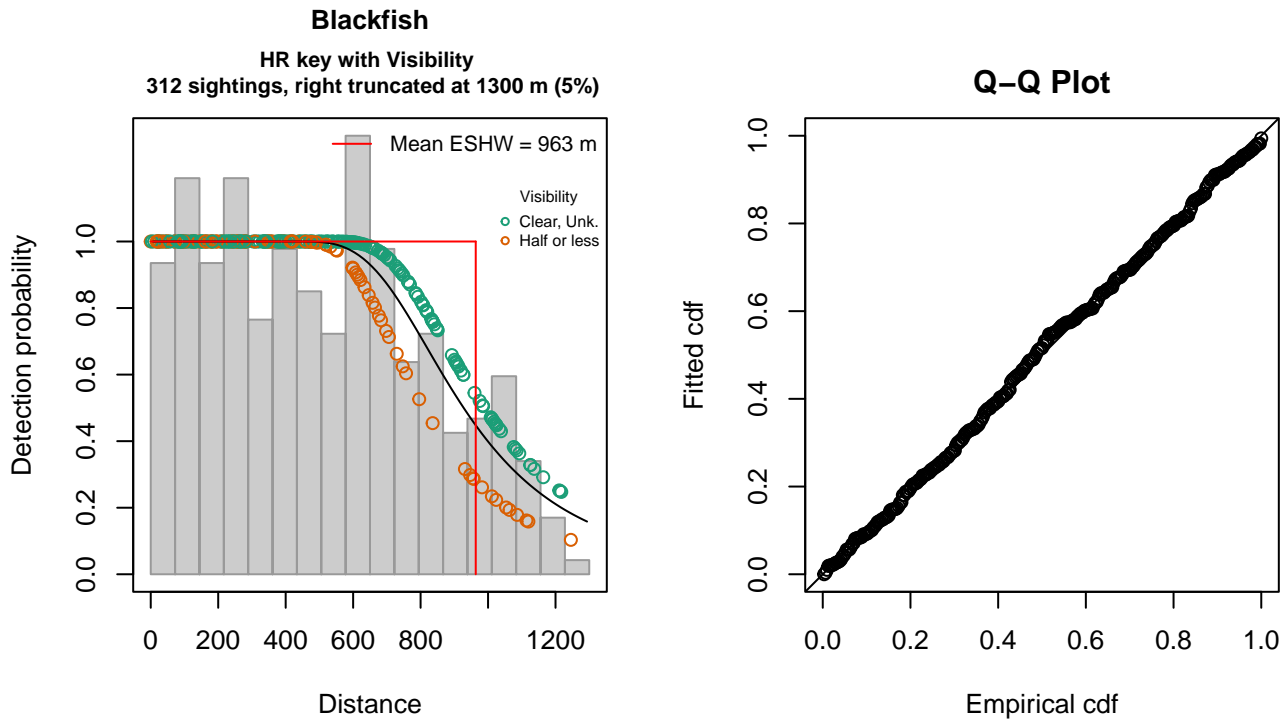


Figure 16: UNCW Navy and VAMSC detection function and Q-Q plot showing its goodness of fit.

Statistical output for this detection function:

Summary for ds object

Number of observations : 312
 Distance range : 0 - 1300
 AIC : 4410.896

Detection function:

Hazard-rate key function

Detection function parameters

Scale coefficient(s):

	estimate	se
(Intercept)	6.8110764	0.06588732
VisibilityHalf or less	-0.1997402	0.10267594

Shape coefficient(s):

	estimate	se
(Intercept)	1.45681	0.2585487

	Estimate	SE	CV
Average p	0.7368436	0.03057513	0.04149473
N in covered region	423.4277360	21.50283164	0.05078277

Distance sampling Cramer-von Mises test (unweighted)

Test statistic = 0.030099 p = 0.975843

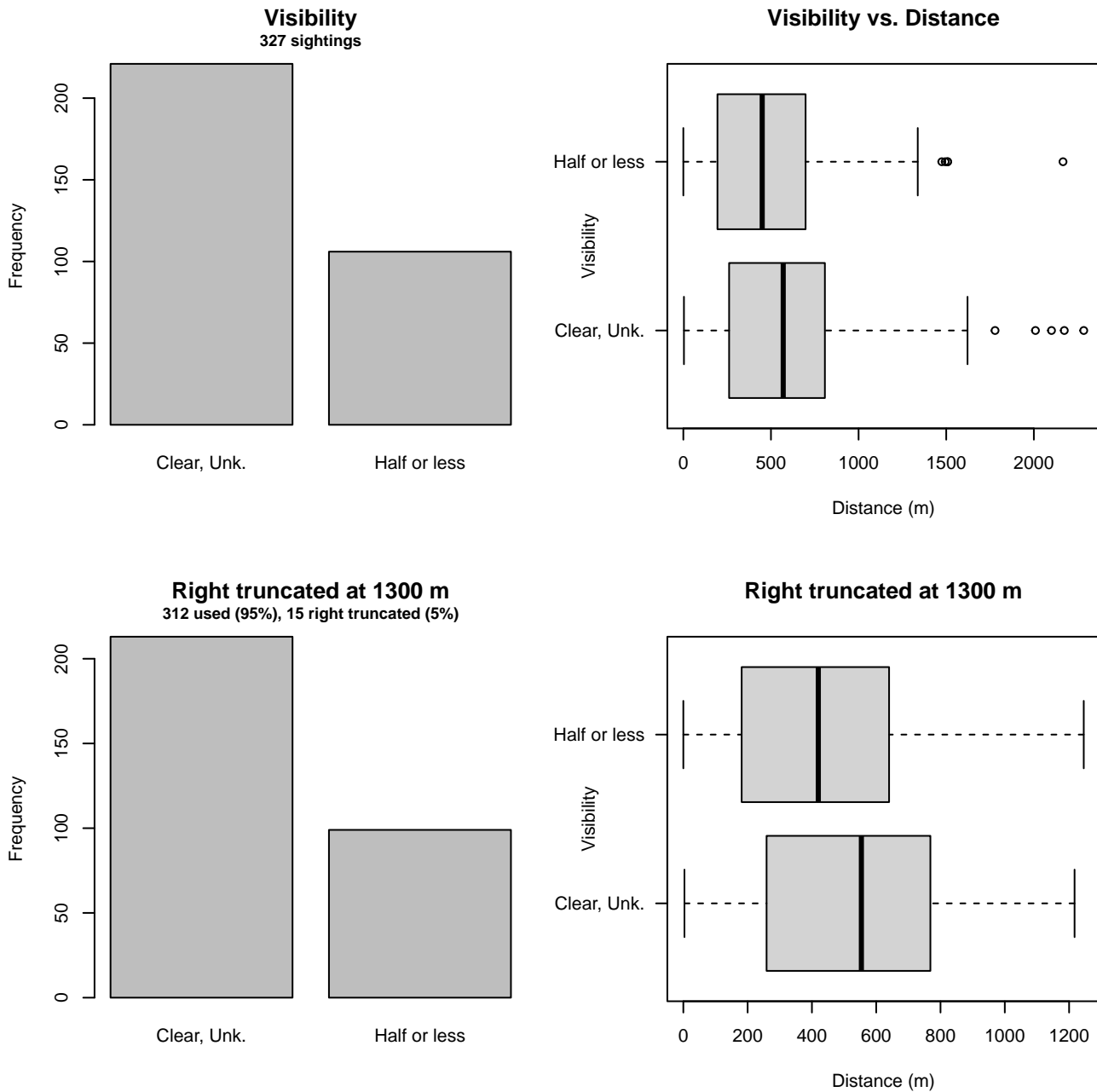


Figure 17: Distribution of the Visibility covariate before (top row) and after (bottom row) observations were truncated to fit the UNCW Navy and VAMSC detection function.

3.1.1.8 HDR

After right-truncating observations greater than 1500 m and left-truncating observations less than 111 m (Figure 19), we fitted the detection function to the 108 observations that remained (Table 12). The selected detection function (Figure 18) used a hazard rate key function with Swell (Figure 20) as a covariate.

Table 12: Observations used to fit the HDR detection function.

ScientificName	n
Globicephala	66
Grampus griseus	42
Total	108

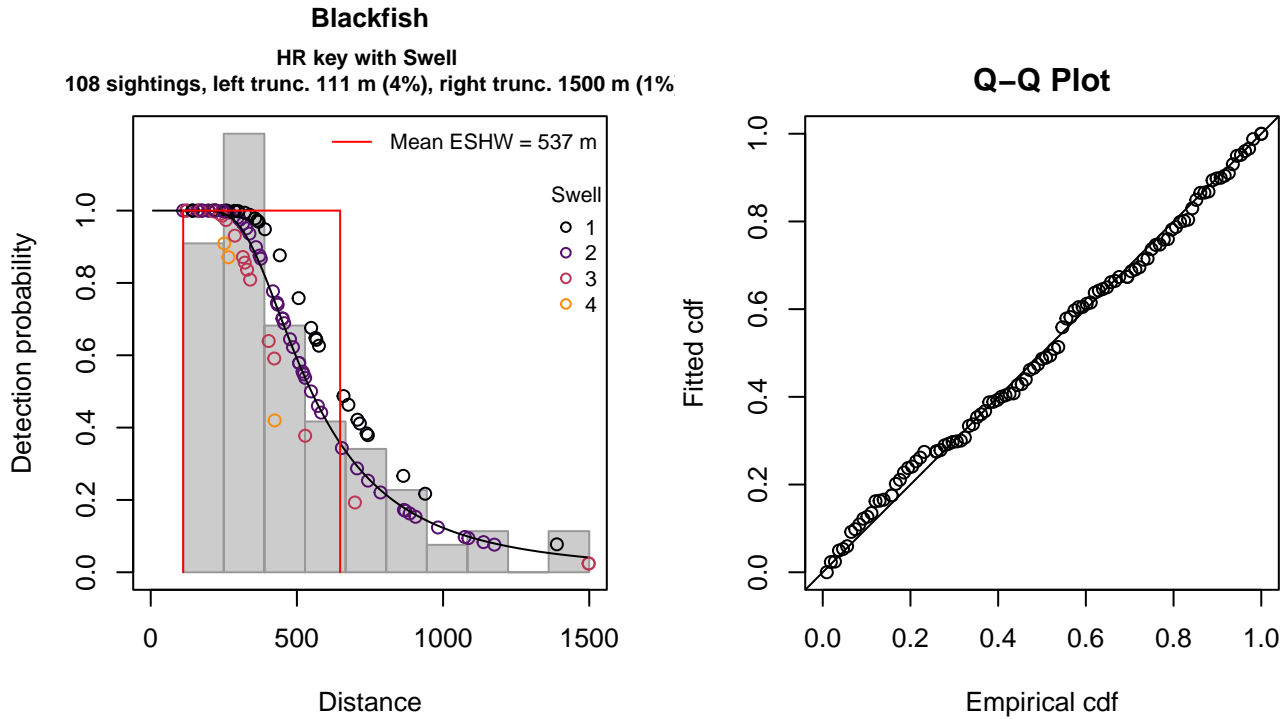


Figure 18: HDR detection function and Q-Q plot showing its goodness of fit.

Statistical output for this detection function:

Summary for ds object

Number of observations : 108
 Distance range : 111 - 1500
 AIC : 1479.102

Detection function:

Hazard-rate key function

Detection function parameters

Scale coefficient(s):

	estimate	se
(Intercept)	6.5207075	0.2852850
Swell	-0.1712662	0.1474231

Shape coefficient(s):

	estimate	se
(Intercept)	1.044626	0.1820091

	Estimate	SE	CV
Average p	0.3789427	0.04750114	0.1253518
N in covered region	285.0035382	41.82280744	0.1467449

Distance sampling Cramer-von Mises test (unweighted)

Test statistic = 0.045799 p = 0.901252

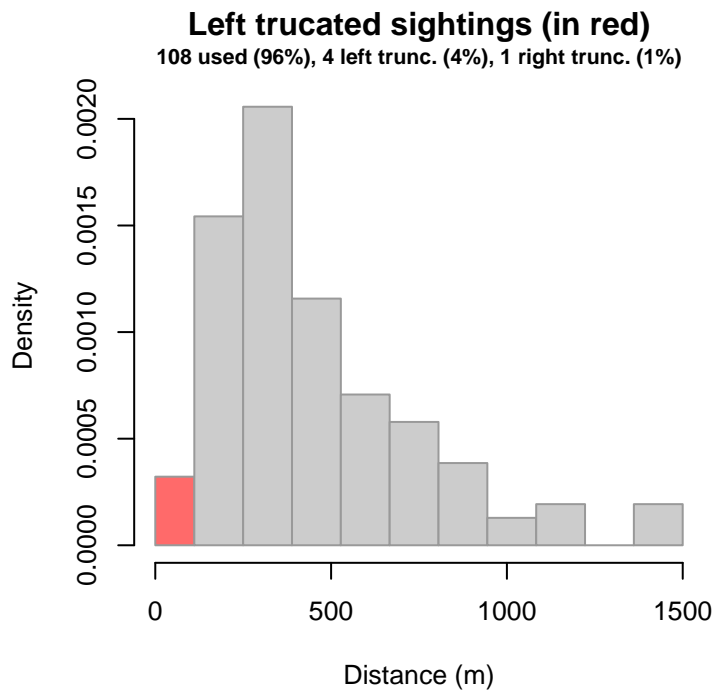


Figure 19: Density histogram of observations used to fit the HDR detection function, with the left-most bar showing observations at distances less than 111 m, which were left-truncated and excluded from the analysis [Buckland et al. (2001)]. (This bar may be very short if there were very few left-truncated sightings, or very narrow if the left truncation distance was very small; in either case it may not appear red.)

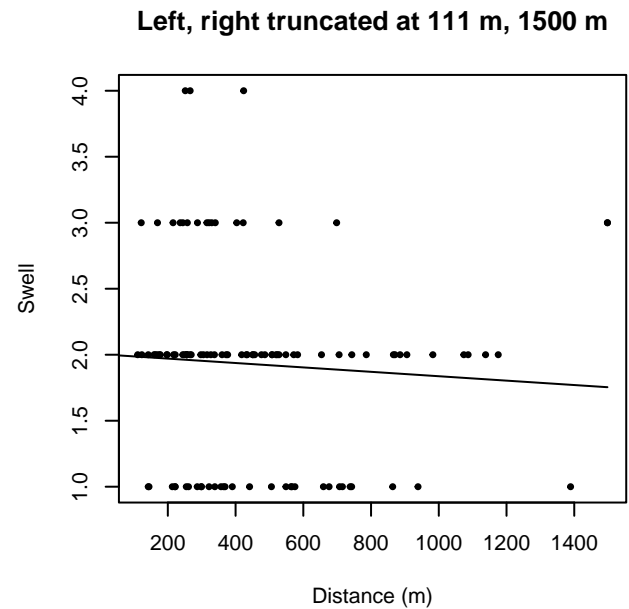
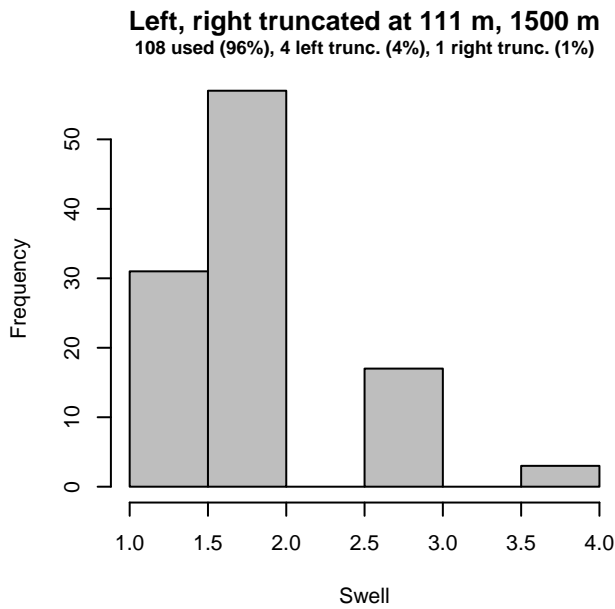
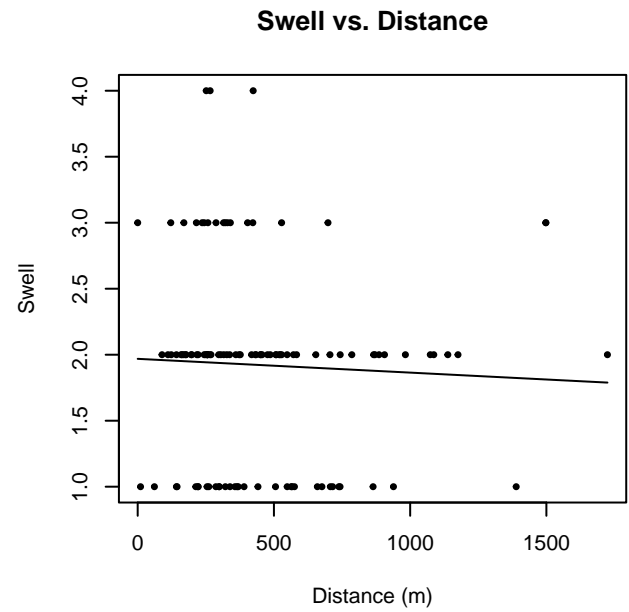
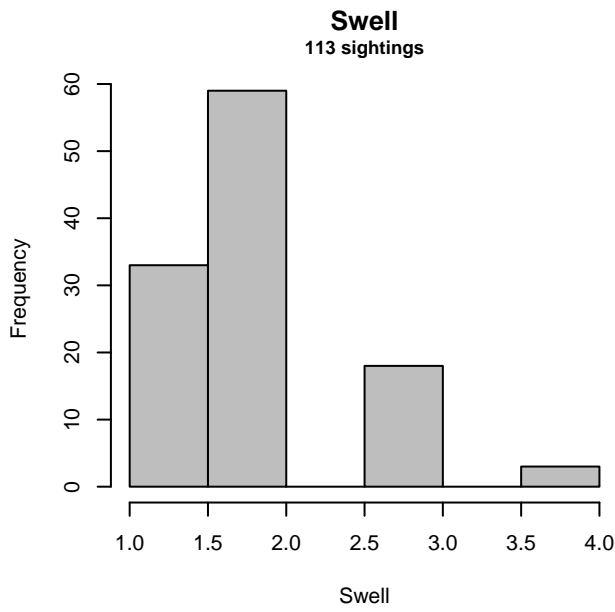


Figure 20: Distribution of the Swell covariate before (top row) and after (bottom row) observations were truncated to fit the HDR detection function.

3.1.2 Shipboard Surveys

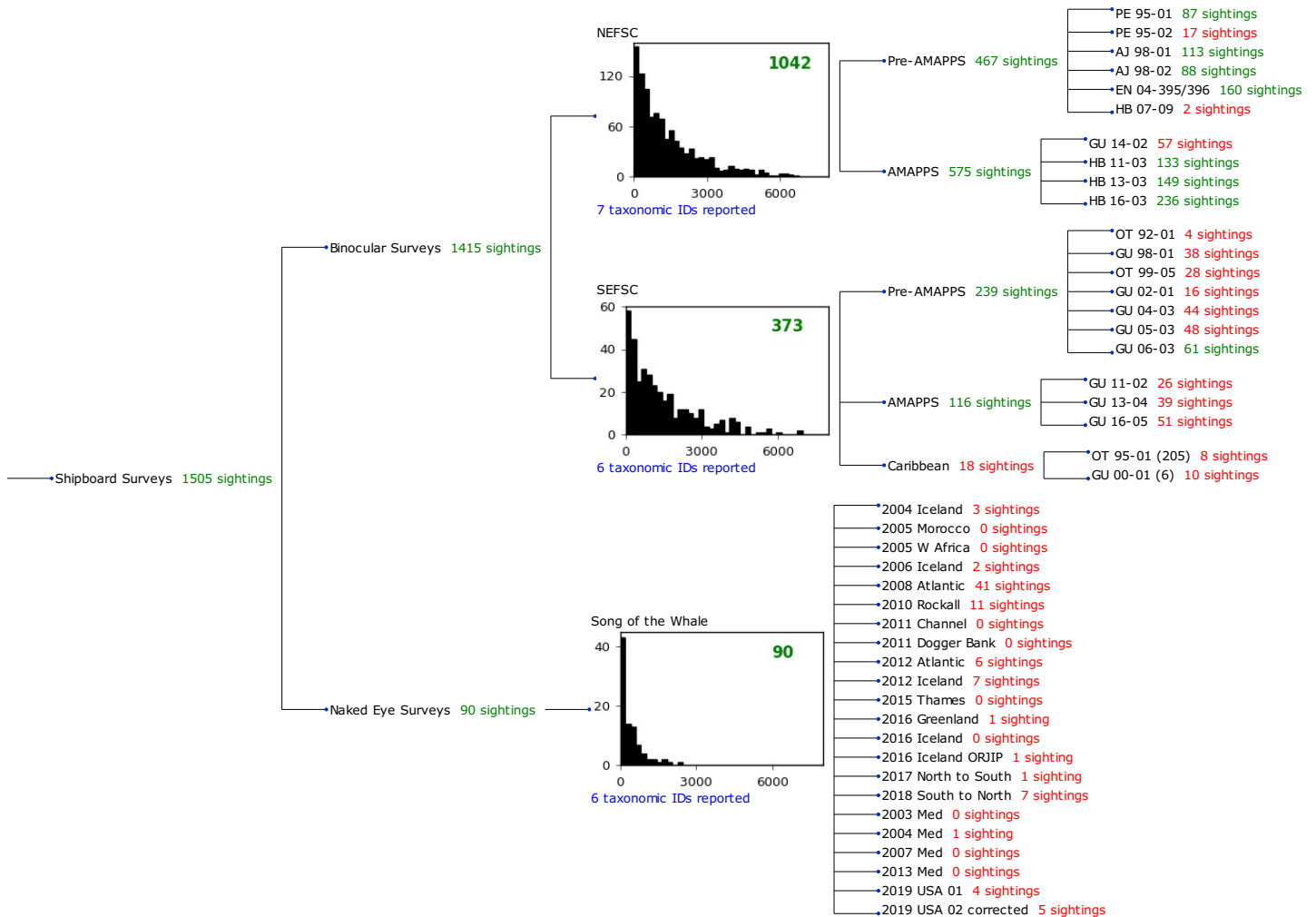


Figure 21: Detection hierarchy for shipboard surveys, showing how they were pooled during detectability modeling, for detection functions that pooled multiple taxa but could not use a taxonomic covariate to account for differences between them. Each histogram represents a detection function and summarizes the perpendicular distances of observations that were pooled to fit it, prior to truncation. Observation counts, also prior to truncation, are shown in green when they met the recommendation of Buckland et al. (2001) that detection functions utilize at least 60 sightings, and red otherwise. For rare taxa, it was not always possible to meet this recommendation, yielding higher statistical uncertainty. During the spatial modeling stage of the analysis, effective strip widths were computed for each survey using the closest detection function above it in the hierarchy (i.e. moving from right to left in the figure). Surveys that do not have a detection function above them in this figure were either addressed by a detection function presented in a different section of this report, or were omitted from the analysis.

3.1.2.1 NEFSC

After right-truncating observations greater than 6500 m, we fitted the detection function to the 1038 observations that remained (Table 13). The selected detection function (Figure 22) used a hazard rate key function with Beaufort (Figure 23), Program (Figure 24) and VesselName (Figure 25) as covariates.

Table 13: Observations used to fit the NEFSC detection function.

ScientificName	n
Feresa attenuata	1
Globicephala	339
Globicephala macrorhynchus	3
Globicephala melas	2
Grampus griseus	687
Orcinus orca	2
Pseudorca crassidens	4
Total	1038

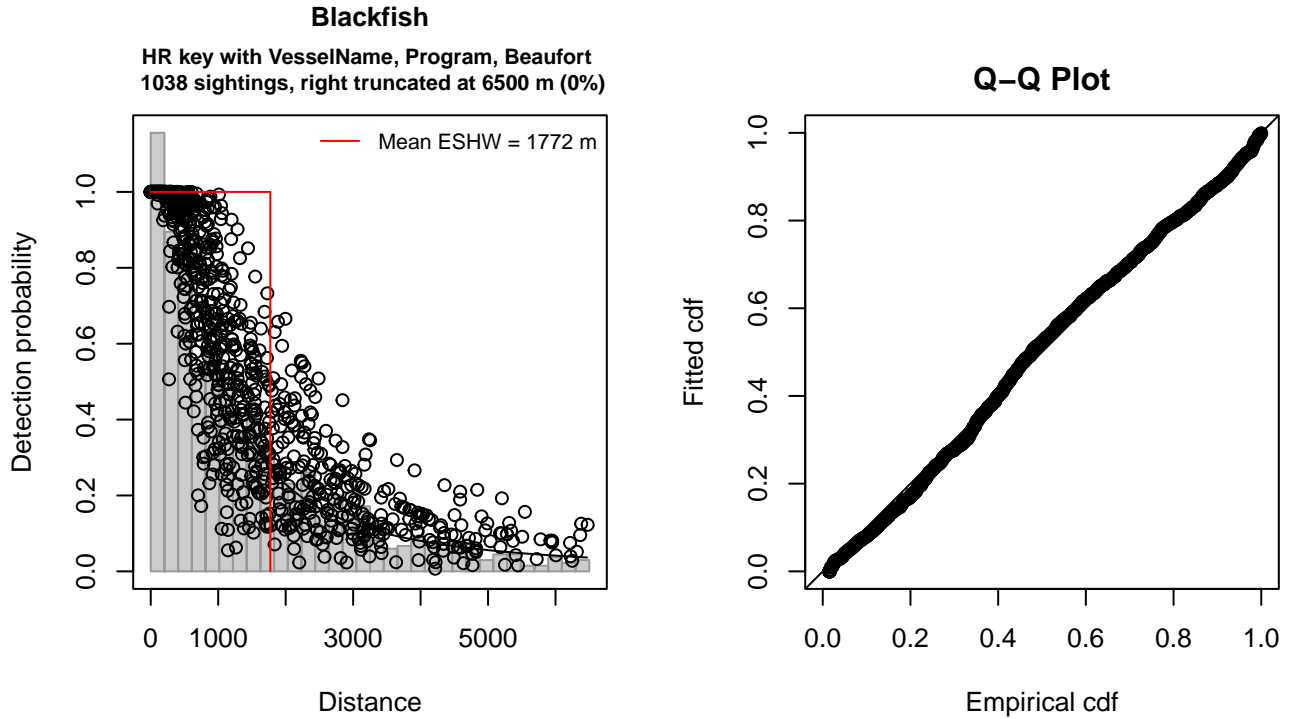


Figure 22: NEFSC detection function and Q-Q plot showing its goodness of fit.

Statistical output for this detection function:

Summary for ds object

Number of observations : 1038
 Distance range : 0 - 6500
 AIC : 17099.06

Detection function:

Hazard-rate key function

Detection function parameters

Scale coefficient(s):

	estimate	se
(Intercept)	7.9293942	0.15761667
VesselNameGunter	-0.8354128	0.20812306
VesselNamePelican	-0.3342984	0.17874334
ProgramMarine Mammal Abundance Surveys	-0.2436275	0.10871377
Beaufort	-0.3461133	0.05534466

Shape coefficient(s):

	estimate	se
(Intercept)	0.5332413	0.05606824

	Estimate	SE	CV
Average p	0.2418497	0.01240714	0.05130104
N in covered region	4291.9212516	249.96005128	0.05823966

Distance sampling Cramer-von Mises test (unweighted)

Test statistic = 0.293125 p = 0.141354

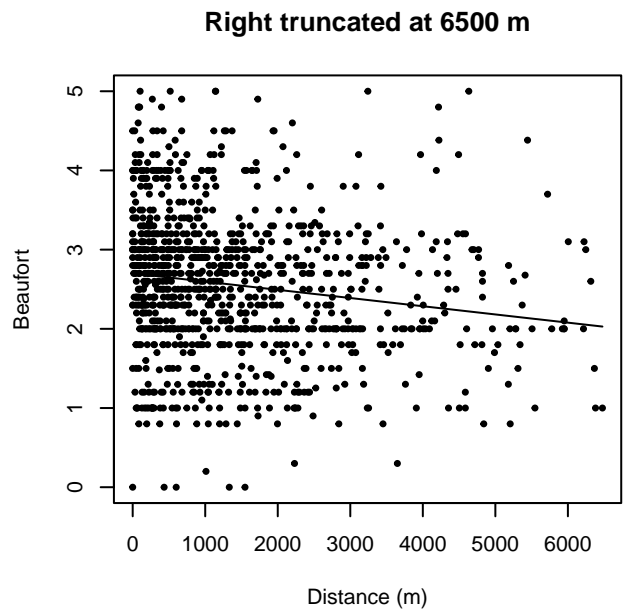
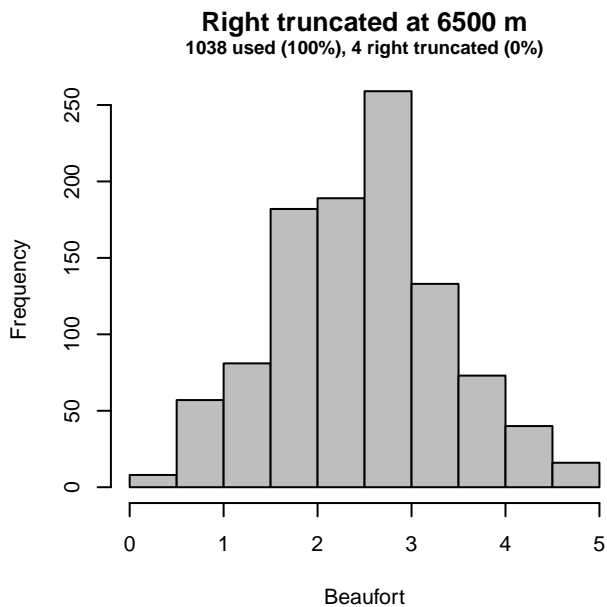
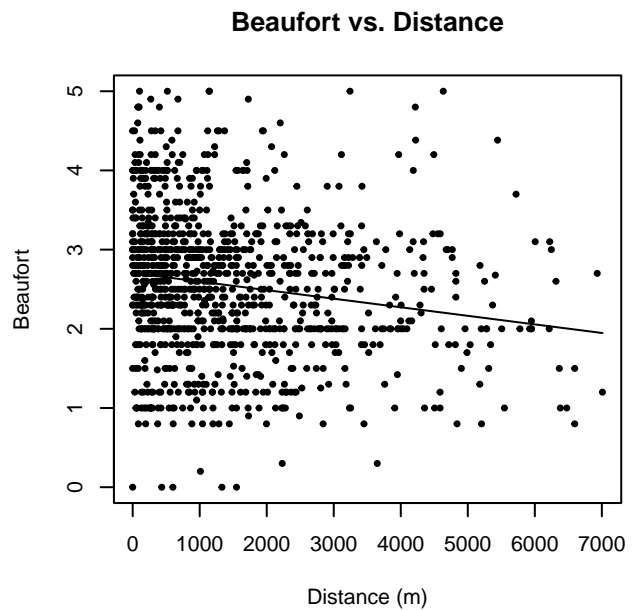
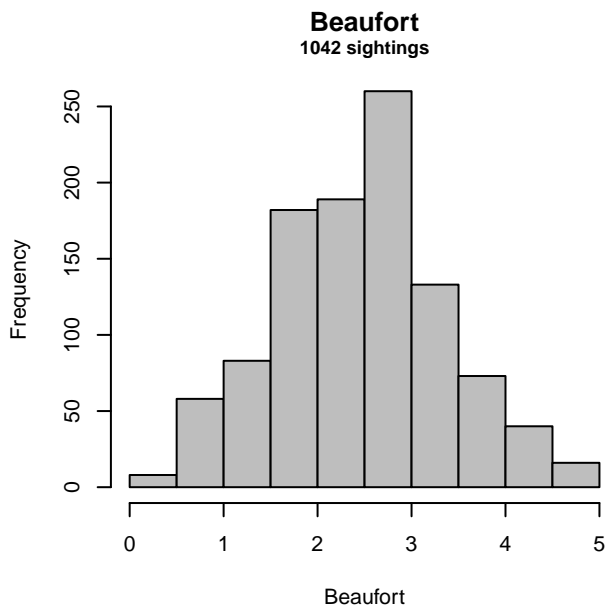


Figure 23: Distribution of the Beaufort covariate before (top row) and after (bottom row) observations were truncated to fit the NEFSC detection function.

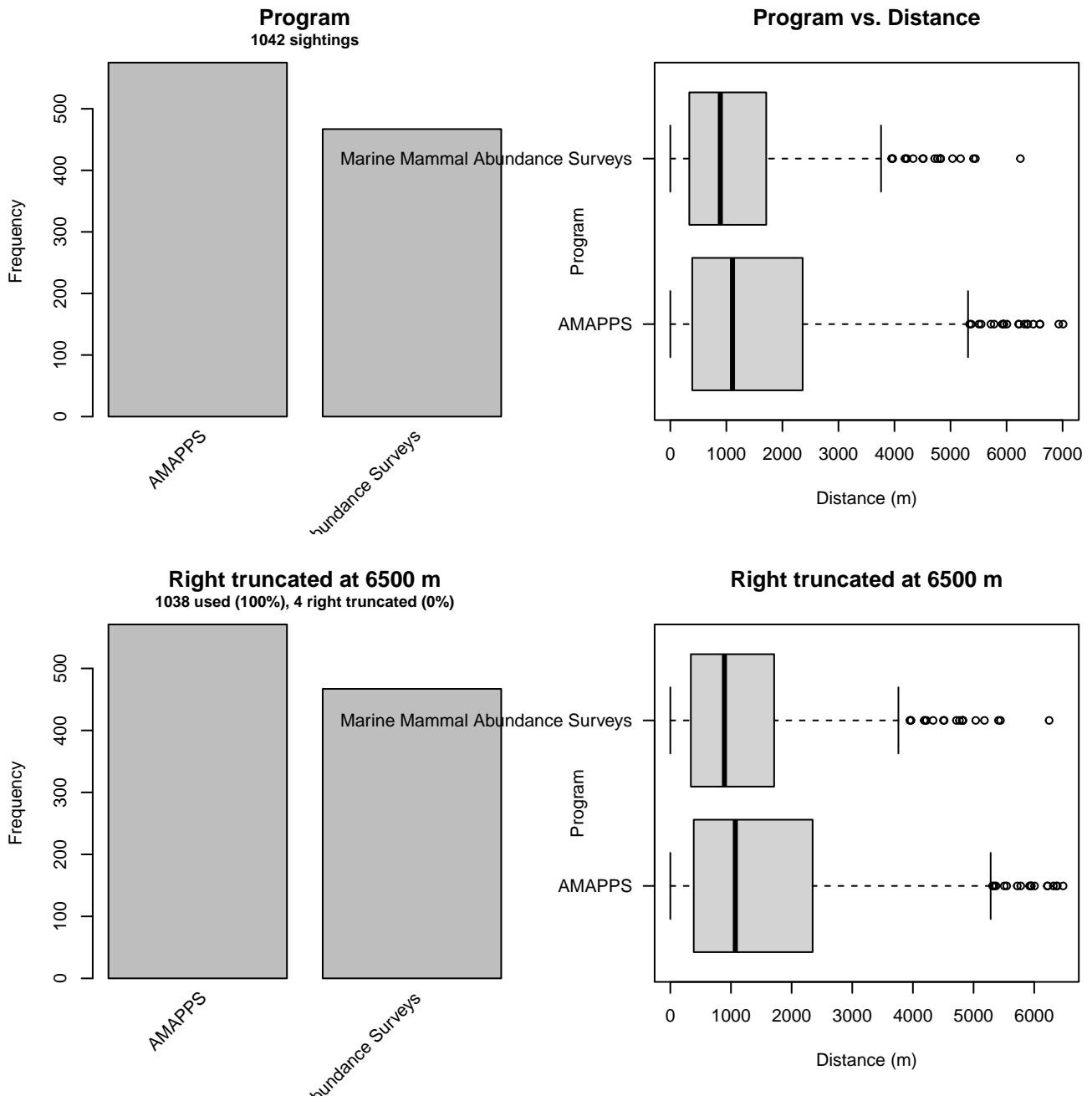


Figure 24: Distribution of the Program covariate before (top row) and after (bottom row) observations were truncated to fit the NEFSC detection function.

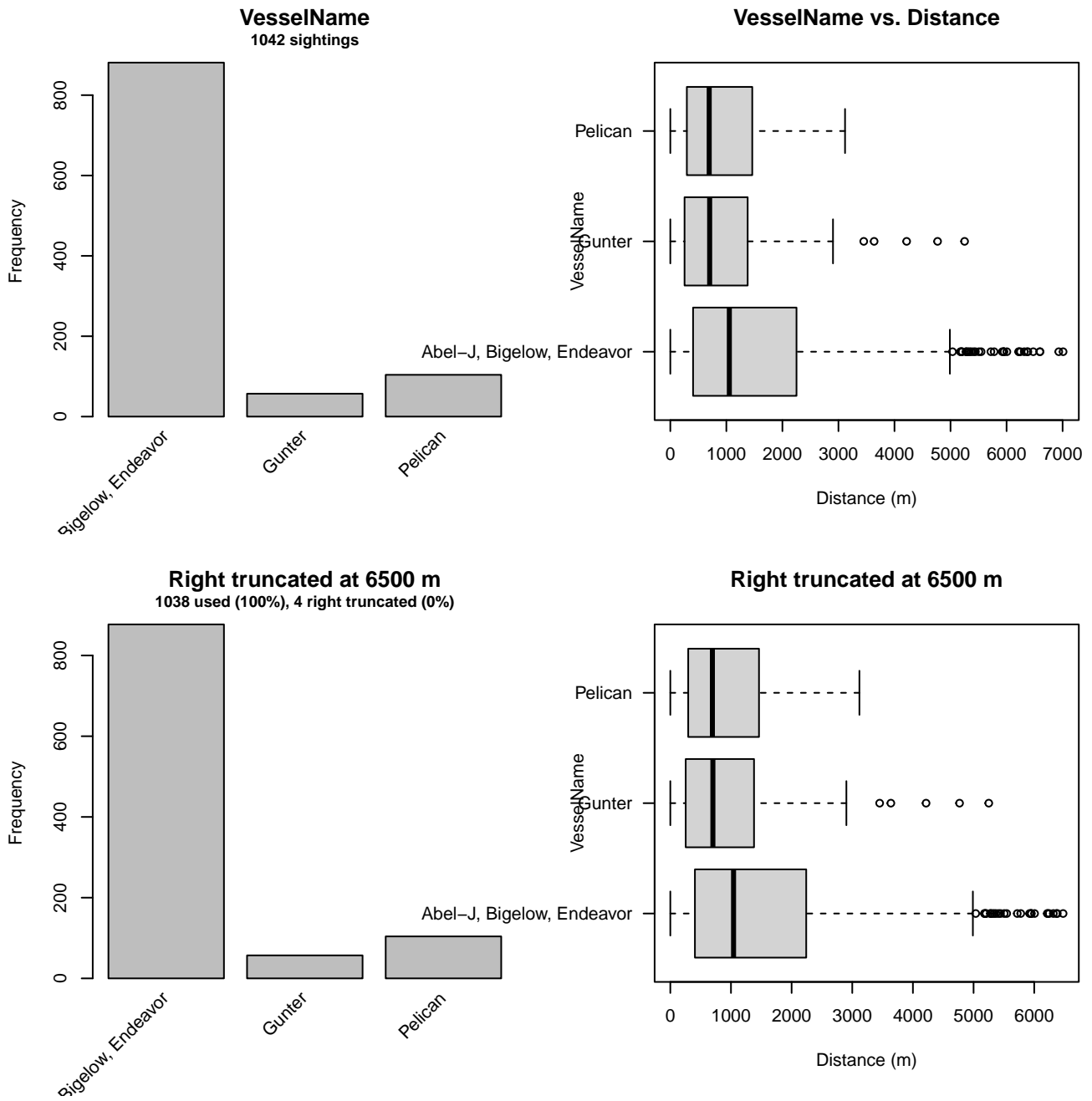


Figure 25: Distribution of the VesselName covariate before (top row) and after (bottom row) observations were truncated to fit the NEFSC detection function.

3.1.2.2 SEFSC

After right-truncating observations greater than 4500 m, we fitted the detection function to the 361 observations that remained (Table 14). The selected detection function (Figure 26) used a hazard rate key function with Beaufort (Figure 27) and VesselName (Figure 28) as covariates.

Table 14: Observations used to fit the SEFSC detection function.

ScientificName	n
Feresa attenuata/Peponocephala electra	7
Globicephala	227
Grampus griseus	121
Orcinus orca	1
Peponocephala electra	3
Pseudorca crassidens	2
Total	361

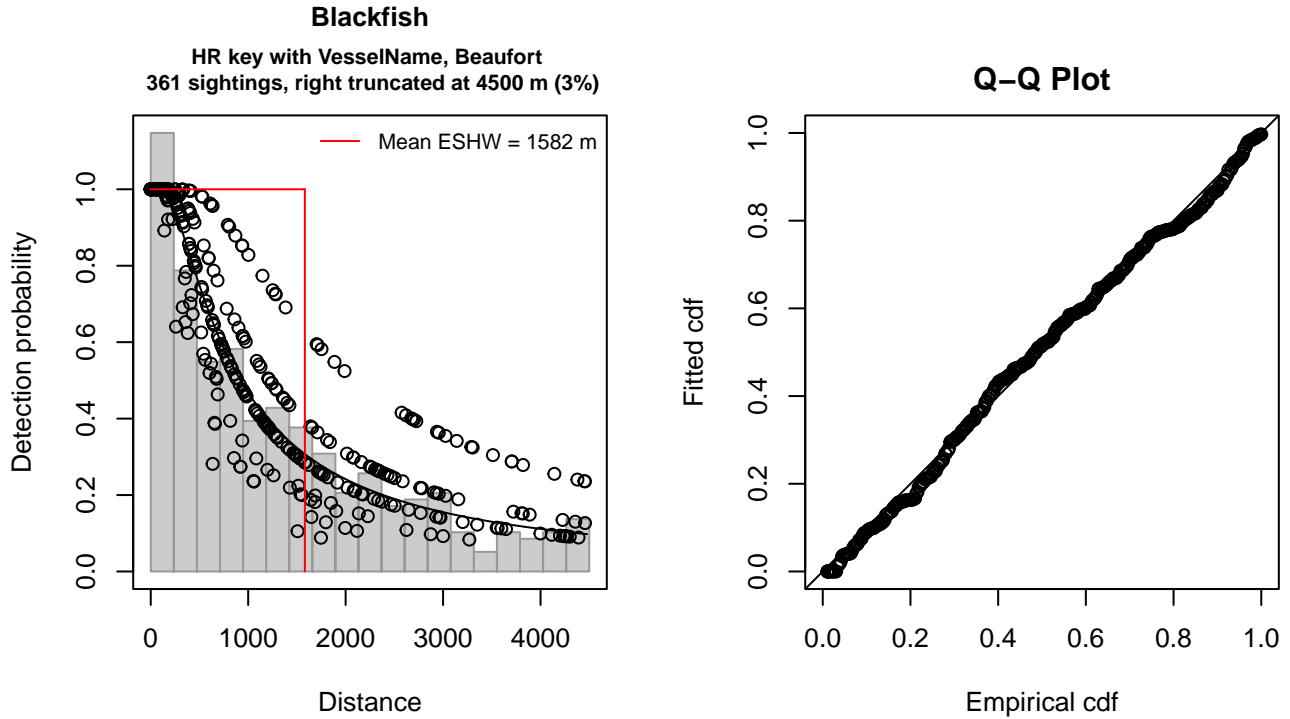


Figure 26: SEFSC detection function and Q-Q plot showing its goodness of fit.

Statistical output for this detection function:

Summary for ds object

Number of observations : 361
 Distance range : 0 - 4500
 AIC : 5876.279

Detection function:

Hazard-rate key function

Detection function parameters

Scale coefficient(s):

	estimate	se
(Intercept)	7.3597538	0.3426685
VesselNameOregon II	-0.5805409	0.4158932
Beaufort2	-0.5439643	0.4011114
Beaufort3-4	-0.8577400	0.3820711
Beaufort5	-1.2038982	0.5170081

Shape coefficient(s):

estimate se
 (Intercept) 0.2309157 0.1254747

	Estimate	SE	CV
Average p	0.3253837	0.03477386	0.1068703
N in covered region	1109.4594048	128.24893603	0.1155959

Distance sampling Cramer-von Mises test (unweighted)
 Test statistic = 0.112666 p = 0.526278

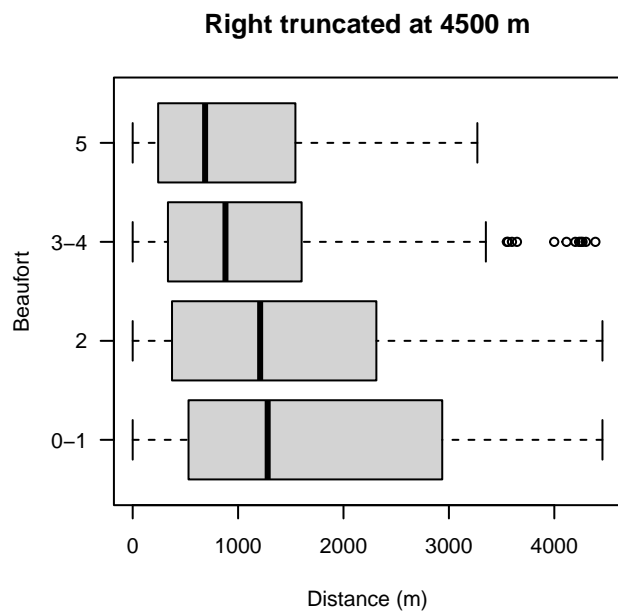
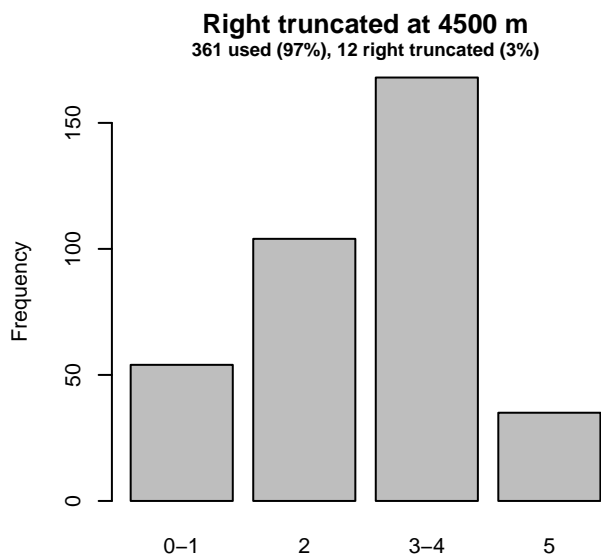
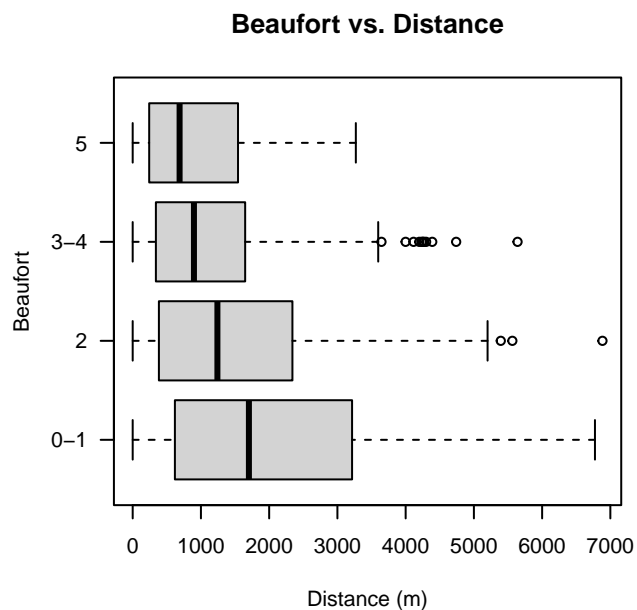
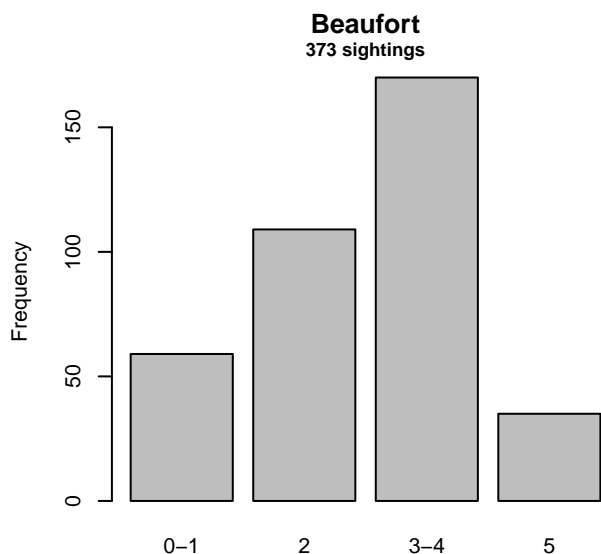


Figure 27: Distribution of the Beaufort covariate before (top row) and after (bottom row) observations were truncated to fit the SEFSC detection function.

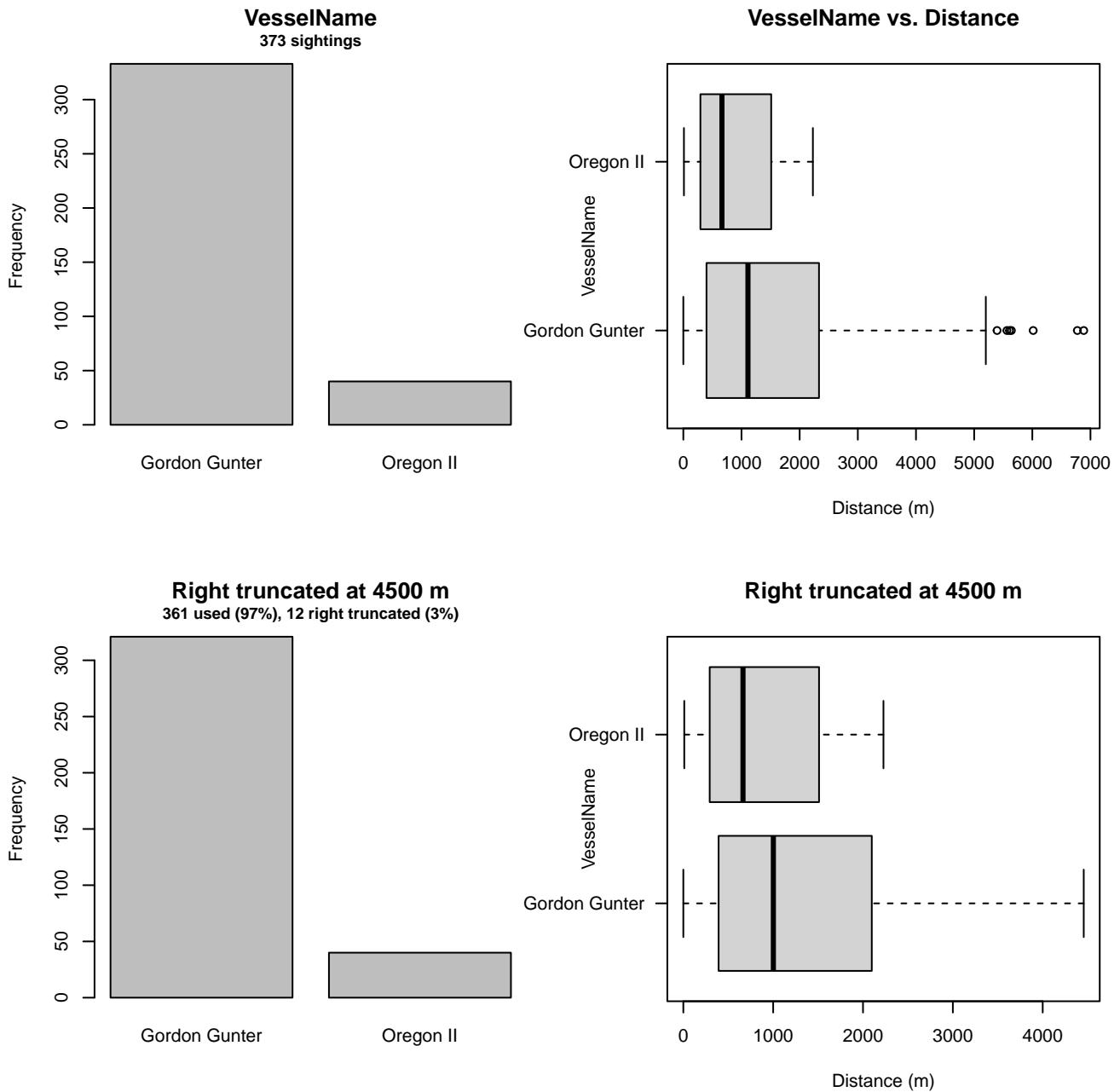


Figure 28: Distribution of the VesselName covariate before (top row) and after (bottom row) observations were truncated to fit the SEFSC detection function.

3.1.2.3 Song of the Whale

After right-truncating observations greater than 1500 m, we fitted the detection function to the 86 observations that remained (Table 15). The selected detection function (Figure 29) used a hazard rate key function with Beaufort (Figure 30) and Clouds (Figure 31) as covariates.

Table 15: Observations used to fit the Song of the Whale detection function.

ScientificName	n
Globicephala	48
Globicephala macrorhynchus	10
Globicephala melas	3
Grampus griseus	15
Orcinus orca	6
Pseudorca crassidens	4
Total	86

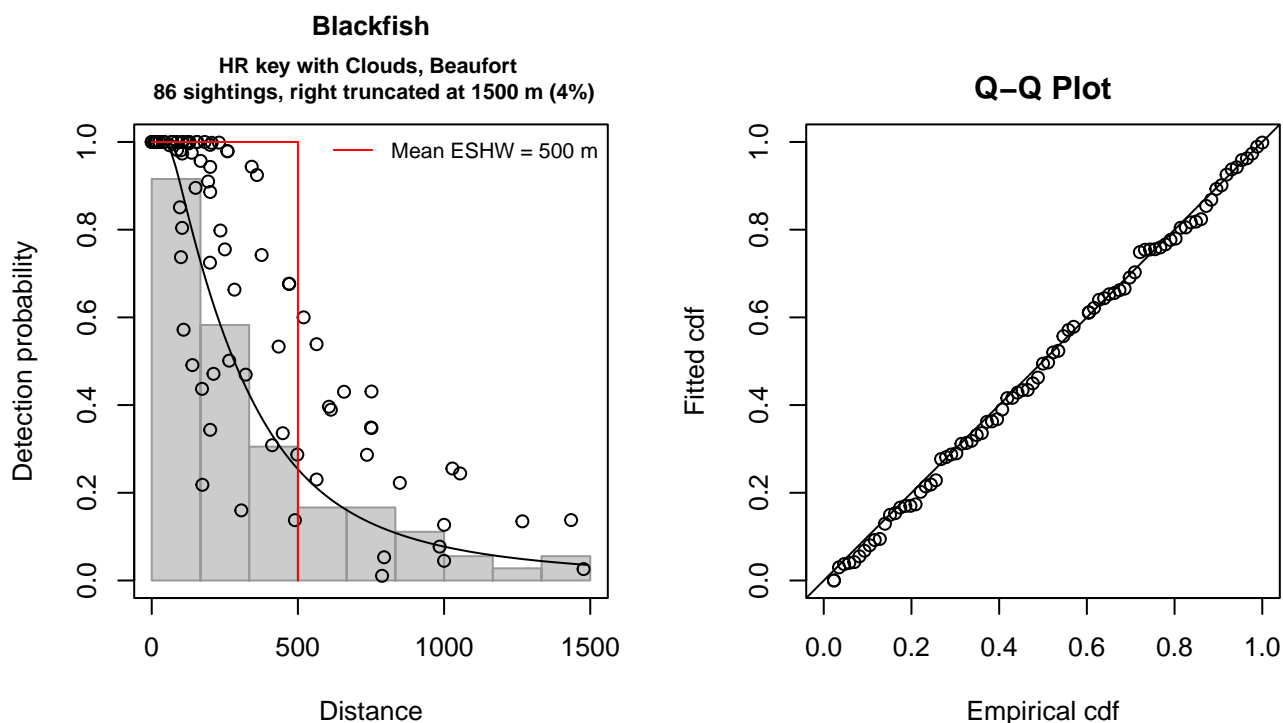


Figure 29: Song of the Whale detection function and Q-Q plot showing its goodness of fit.

Statistical output for this detection function:

Summary for ds object

Number of observations : 86
 Distance range : 0 - 1500
 AIC : 1170.598

Detection function:

Hazard-rate key function

Detection function parameters

Scale coefficient(s):

	estimate	se
(Intercept)	6.4796997	0.26905817
Clouds	-0.1344265	0.04822789
Beaufort3-4	-0.6588095	0.31406041

Shape coefficient(s):

	estimate	se
(Intercept)	0.7265327	0.1798353

	Estimate	SE	CV
Average p	0.265116	0.04508089	0.1700421
N in covered region	324.386340	63.44454836	0.1955833

Distance sampling Cramer-von Mises test (unweighted)
 Test statistic = 0.019751 p = 0.997226

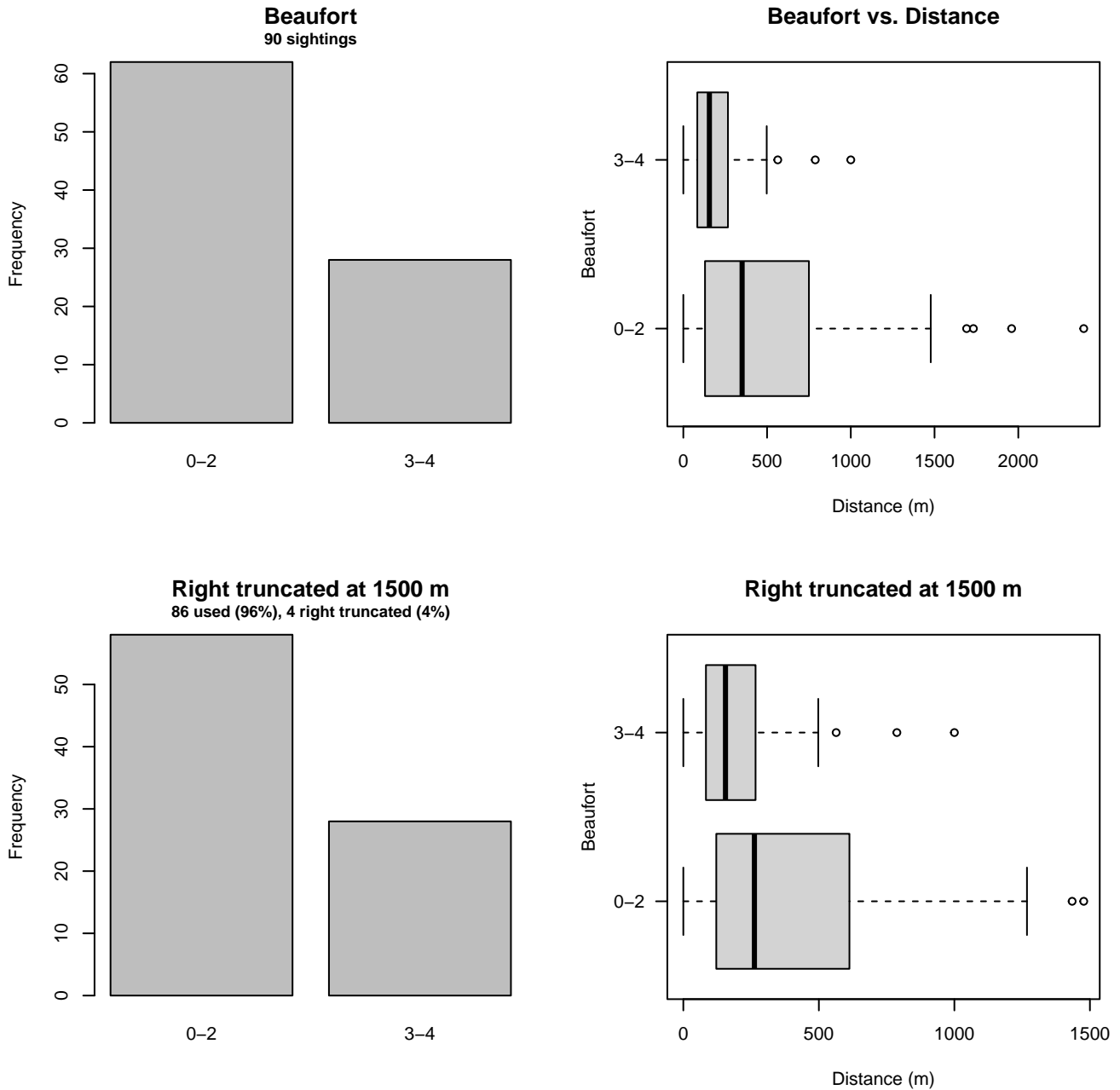


Figure 30: Distribution of the Beaufort covariate before (top row) and after (bottom row) observations were truncated to fit the Song of the Whale detection function.

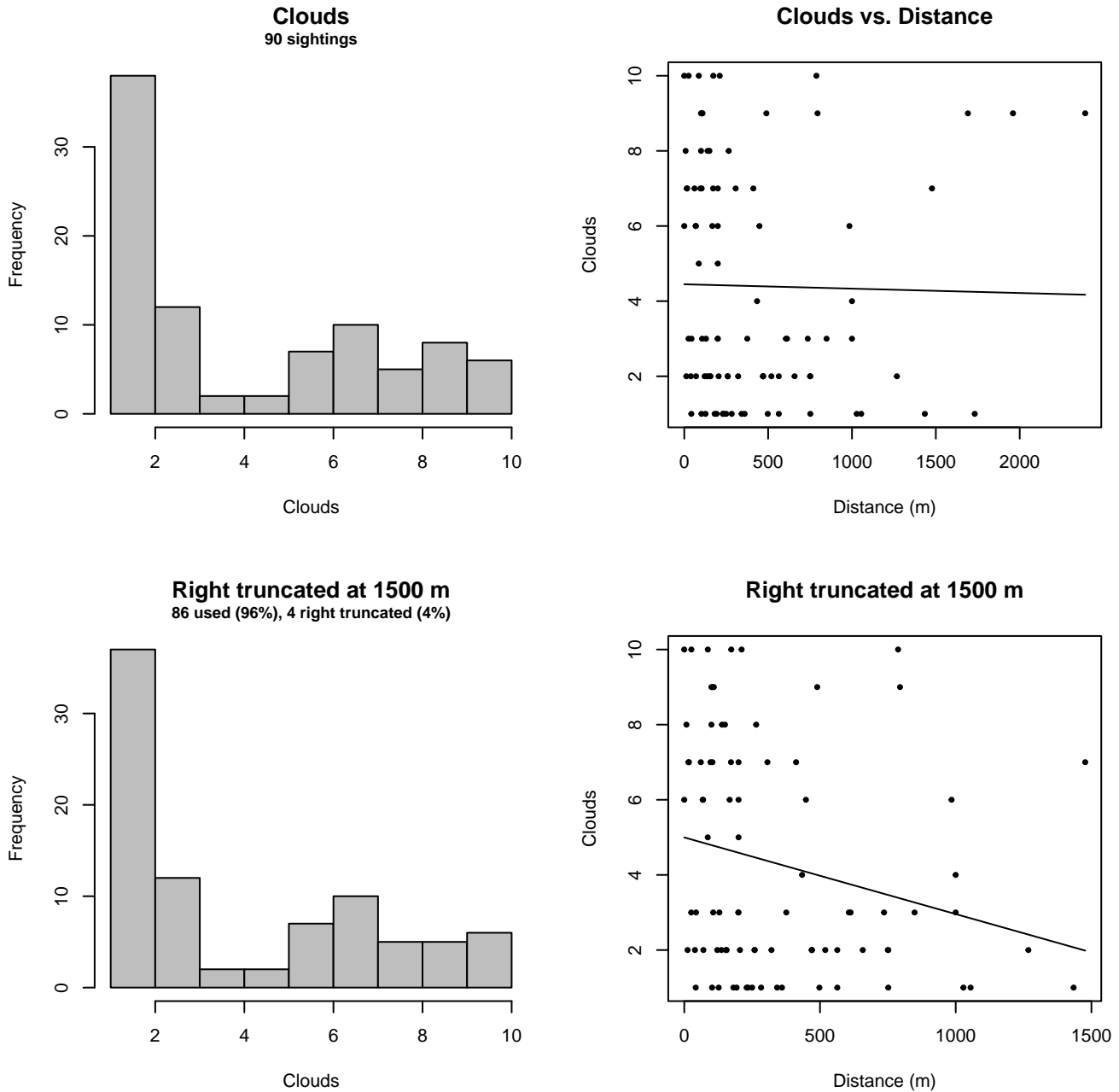


Figure 31: Distribution of the Clounds covariate before (top row) and after (bottom row) observations were truncated to fit the Song of the Whale detection function.

4 Bias Corrections

Density surface modeling methodology uses *distance sampling* (Buckland et al. 2001) to model the probability that an observer on a line transect survey will detect an animal given the perpendicular distance to it from the transect line. Distance sampling assumes that detection probability is 1 when perpendicular distance is 0. When this assumption is not met, detection probability is biased high, leading to an underestimation of density and abundance. This is known as the $g_0 < 1$ problem, where g_0 refers to the detection probability at distance 0. Modelers often try to address this problem by estimating g_0 empirically and dividing it into estimated density or abundance, thereby correcting those estimates to account for the animals that were presumed missed.

Two important sources of bias for visual surveys are known as *availability bias*, in which an animal was present on the transect line but impossible to detect, e.g. because it was under water, and *perception bias*, in which an animal was present and available but not noticed, e.g. because of its small size or cryptic coloration or behavior (Marsh and Sinclair 1989). Modelers often

estimate the influence of these two sources of bias on detection probability independently, yielding two estimates of g_0 , hereafter referred to as g_{0A} and g_{0P} , and multiply them together to obtain a final, combined estimate: $g_0 = g_{0A} \cdot g_{0P}$.

Our overall approach was to perform this correction on a per-observation basis, to have the flexibility to account for many factors such as platform type, surveyor institution, group size, group composition (e.g. singleton, mother-calf pair, or surface active group), and geographic location (e.g. feeding grounds vs. calving grounds). The level of complexity of the corrections varied by species according to the amount of information available, with North Atlantic right whale having the most elaborate corrections, derived from a substantial set of publications documenting its behavior, and various lesser known odontocetes having corrections based only on platform type (aerial or shipboard), derived from comparatively sparse information. Here we document the corrections used for melon-headed whale.

4.1 Aerial Surveys

Only one aerial sighting of this rare species was retained for analysis, a group of 185 melon-headed whales sighted by UNCW on 14 March 2011 at the shelf break off Cape Hatteras. UNCW reported a second sighting of 210 whales the next day 23 km away, likely the same group, but this sighting was right-truncated. To the one sighting that was retained, we applied the perception bias correction factor of Carretta et al. (2000) for groups of more than 25 delphinids: $g_{0P} = 0.994$.

Our usual practice for estimating availability bias was to apply, on a per-sighting basis, the Laake et al. (1997) estimator, which requires the use of dive and surface intervals. West et al. (2018) reported median daytime dive intervals of 4-5 minutes for three melon-headed whales in Hawaii tracked with LIMPET tags. Although these intervals are relatively long for a small cetacean, this was of little consequence because the next step was to apply the group availability estimator of McLellan et al. (2018). The group availability estimator assumes the individuals in the group dive asynchronously. Under this assumption, for a group of 75 animals, $g_{0A} > 0.999$, even for the longest diving animals, for which the single animal estimate might be $g_{0A} = 0.1$. Therefore we assumed that $g_{0A} = 1$ for this group of 185.

4.2 Shipboard Surveys

Two shipboard sightings were reported, both by SEFSC. One had a group size of 20. To this sighting, we applied the only correction we were able to locate that had been prepared by our collaborators, in this case by Garrison et al. (in prep), who developed a perception bias correction for a “blackfish” guild that included melon-headed whale, using two team, MRDS methodology (Burt et al. 2014) for high-power binocular surveys conducted in 2003-2018 by SEFSC during the Gulf of Mexico Marine Assessment Program for Protected Species (GoMMAPPS) and predecessor campaigns (Table 16). To the other sighting, which had a group size of 80, we applied the perception bias correction factor of Barlow and Forney (2007) for groups of 21 or more delphinids: $g_{0P} = 0.97$.

The median daytime dive interval of 4-5 minutes reported by West et al. (2018) was short relative to the amount of time a given patch of water remained in view to shipboard observers, and therefore that no availability bias correction was needed ($g_{0A} = 1$).

Table 16: Perception and availability bias corrections for melon-headed whale applied to shipboard surveys.

Surveys	Searching Method	Group Size	g_{0P}	g_{0P} Source	g_{0A}	g_{0A} Source
All	Binoculars	≤ 20	0.6415	Garrison et al. (in prep.)	1	Assumed
All	Binoculars	> 20	0.9700	Barlow and Forney (2007)	1	Assumed

5 Geographic Strata

With so few sightings, it was not possible to fit a traditional density surface model that related density observed on survey segments to environmental covariates. Nor was it possible to make proper design-based abundance estimates using traditional distance sampling (Buckland et al. 2001), because the aggregate surveys provided very heterogeneous coverage that did not together constitute a proper systematic survey design.

To provide interested parties with at least rough estimates of density in ecologically relevant geographic strata, we first split the study area into five strata (Figure 1) at major habitat boundaries. We placed our first split at the continental shelf break, defined as the 100 meter isobath, separating the study area in into shelf and offshore regions. (We manually cut across the Northeast Channel of the Gulf of Maine, so that the Gulf was considered part of the shelf.) We then split the shelf region

at Cape Hatteras, a location where the Gulf Stream separates from the continental shelf, which has previously been used to delineate community structure in marine mammals (Schick et al. 2011). We also split the shelf region at the Nantucket Shoals, which separate the Gulf of Maine from the New York Bight. We split off the bays and sounds of New York, Rhode Island, and southern Massachusetts, generally at the 10 m isobath, on the basis that these inshore areas are rarely visited by cetaceans of any species. Finally, we split the offshore region at the north wall of the Gulf Stream, starting at Cape Hatteras and extending along the north wall of the Gulf Stream, as defined with a long-term climatology of total kinetic energy, to the edge of the study area.

We then derived density estimates for each stratum by fitting a model with no covariates, under the assumption that density would be distributed uniformly within the stratum. This assumption, if true, would mean we would obtain similar density estimates for a given stratum under any sampling design, and therefore it would not matter if there was some heterogeneity in sampling within the stratum. However, we strongly caution that this assumption did not hold for the other, more-common species we successfully modeled with traditional density surface modeling, as evidenced by the non-uniform patterns in density predicted by those species' models. That said, when those results are viewed at a very coarse, ecoregional scale, the boundaries used here often correlate with boundaries or strong gradients in density in those models. Thus, for the much rarer species, such as melon-headed whale documented here, we offer this simplified approach as a rough-and-ready substitute for a full density surface model.

In this section, we present maps of each stratum that contained sightings, with tallies of effort and sightings that occurred.

5.1 Offshore Gulf Stream and South

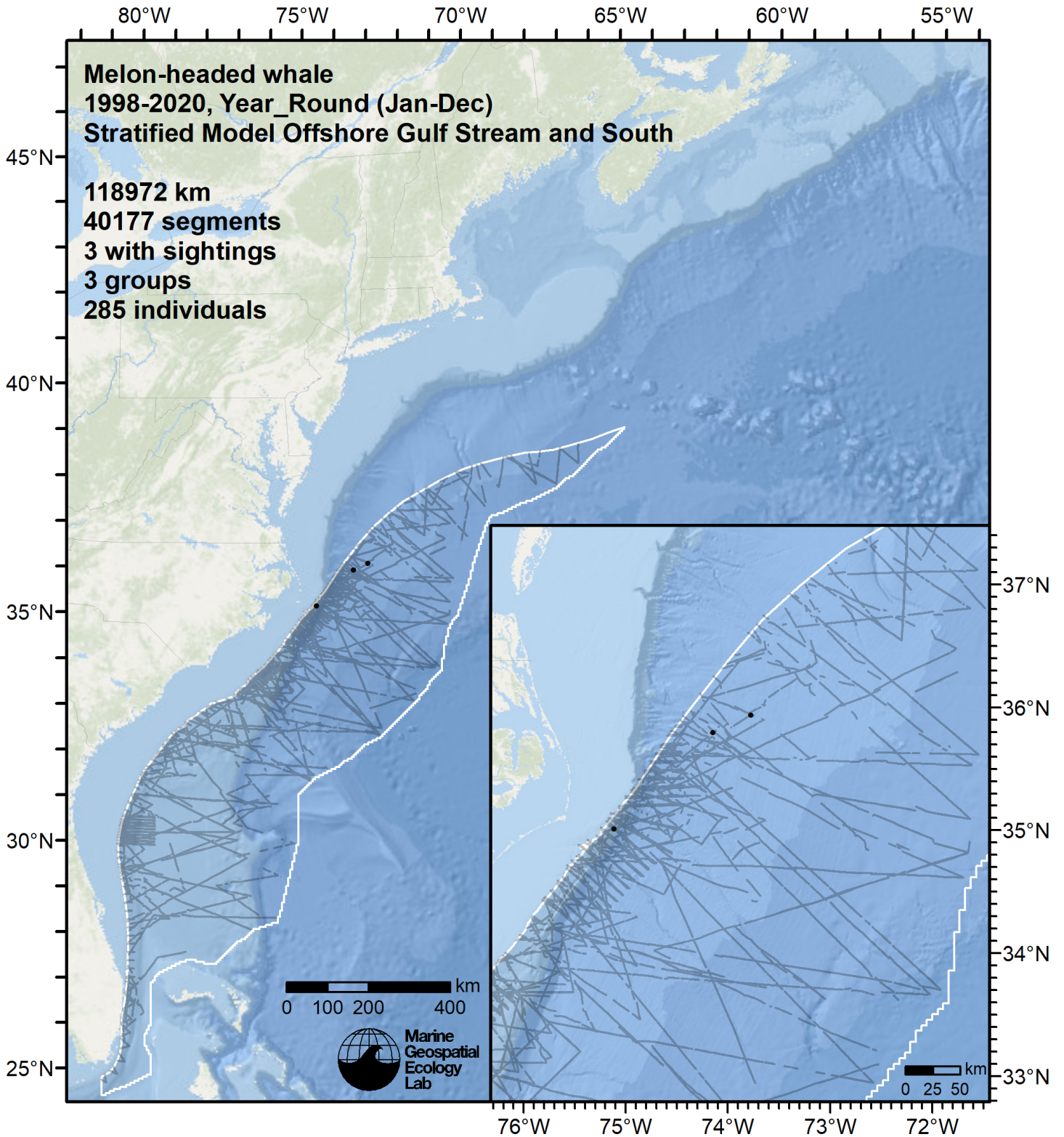


Figure 32: Survey segments and sightings used to estimate melon-headed whale density for the "Offshore Gulf Stream and South" region. Black points indicate segments with observations.

6 Predictions

6.1 Summarized Predictions

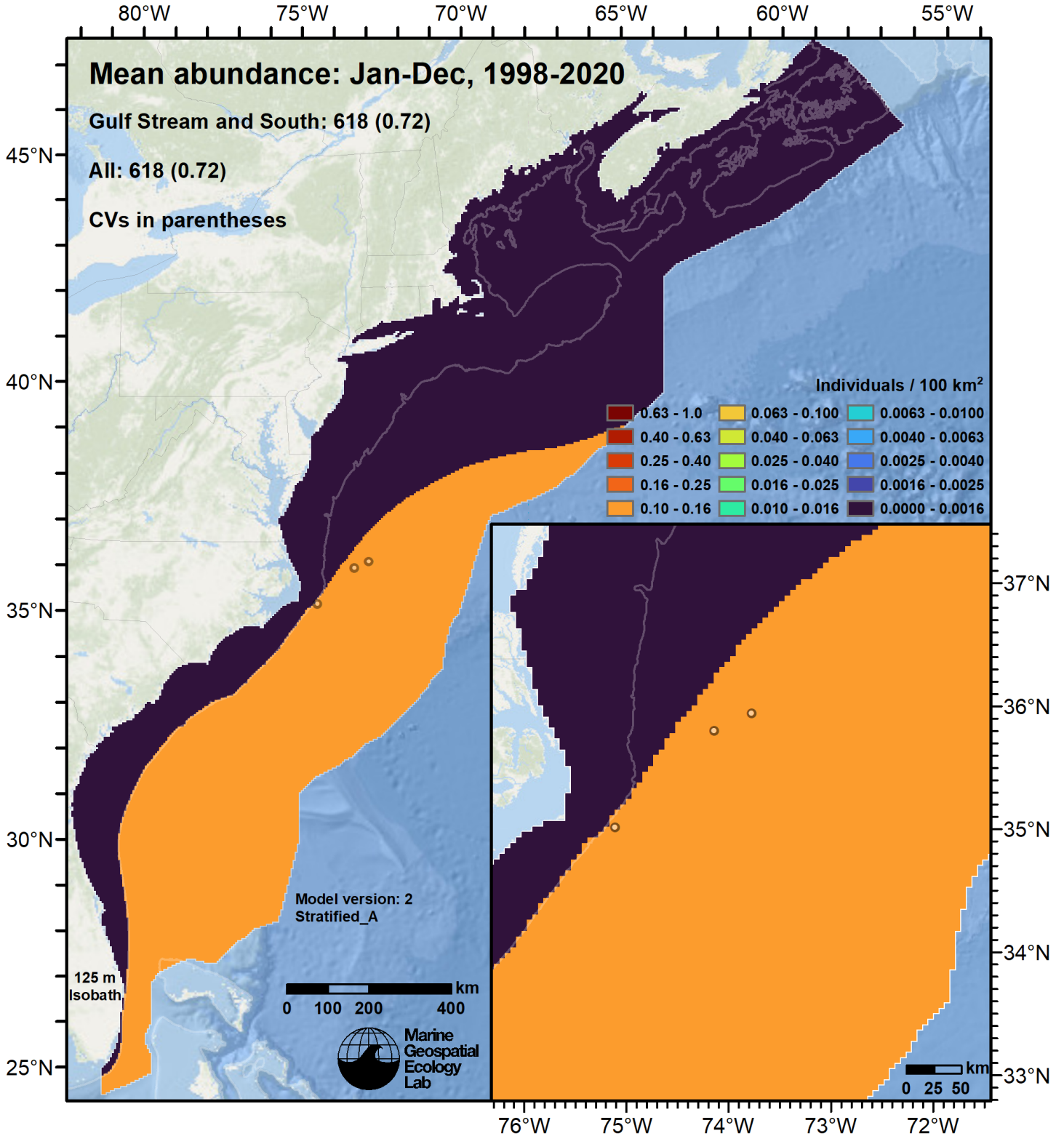


Figure 33: Melon-headed whale density estimated for the indicated period. Open circles indicate segments with observations. The abundance estimate and its coefficient of variation (CV) are given in the subtitle.

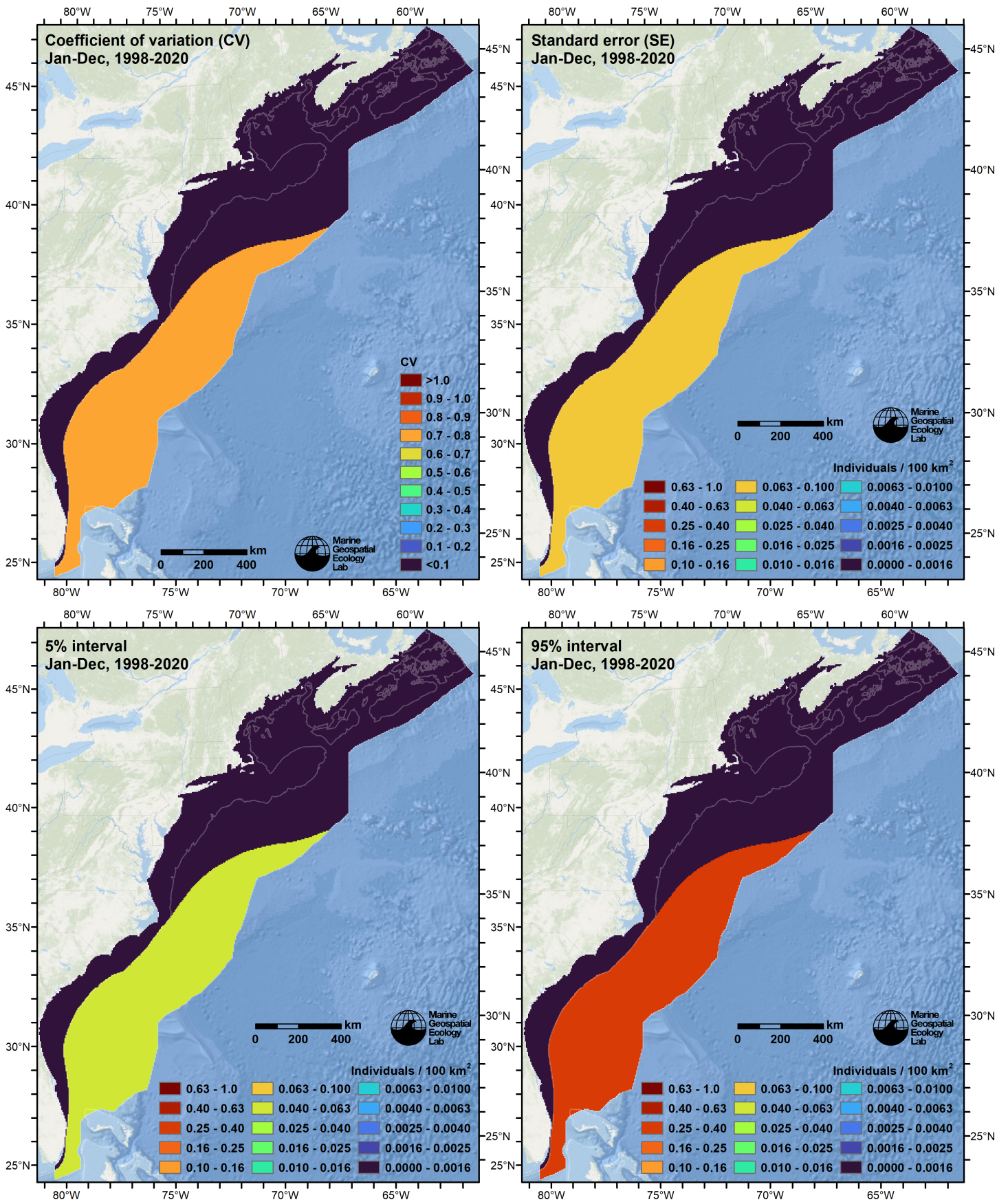


Figure 34: Uncertainty statistics for the melon-headed whale estimated density surface (Figure 33).

Table 17: Melon-headed whale abundance and density estimated for each stratum.

Region	Abundance	CV	95% Interval	Area (km ²)	Density (indiv. / 100 km ²)
Offshore Gulf Stream and South	618	0.72	174 - 2,194	499,300	0.124
Offshore North of Gulf Stream	0	0.00	0 - 0	253,575	0.000
Shelf Cape Hatt. to Nant. Shoals	0	0.00	0 - 0	104,425	0.000
Shelf North of Nantucket Shoals	0	0.00	0 - 0	302,025	0.000
Shelf South of Cape Hatteras	0	0.00	0 - 0	105,500	0.000
Sounds of NY, RI, and MA	0	0.00	0 - 0	8,600	0.000
Total	618	0.72	174 - 2,194	1,273,425	0.049

6.2 Abundance Comparisons

6.2.1 NOAA Stock Assessment Report

The 2019 Stock Assessment Report (SAR) is the most recent to examine melon-headed whale (Hayes et al. 2020), and reports “The number of melon-headed whales off the U.S. Atlantic coast is unknown because they were rarely seen in any surveys.” Thus, no SAR estimate is available for comparison.

6.2.2 Previous Density Model

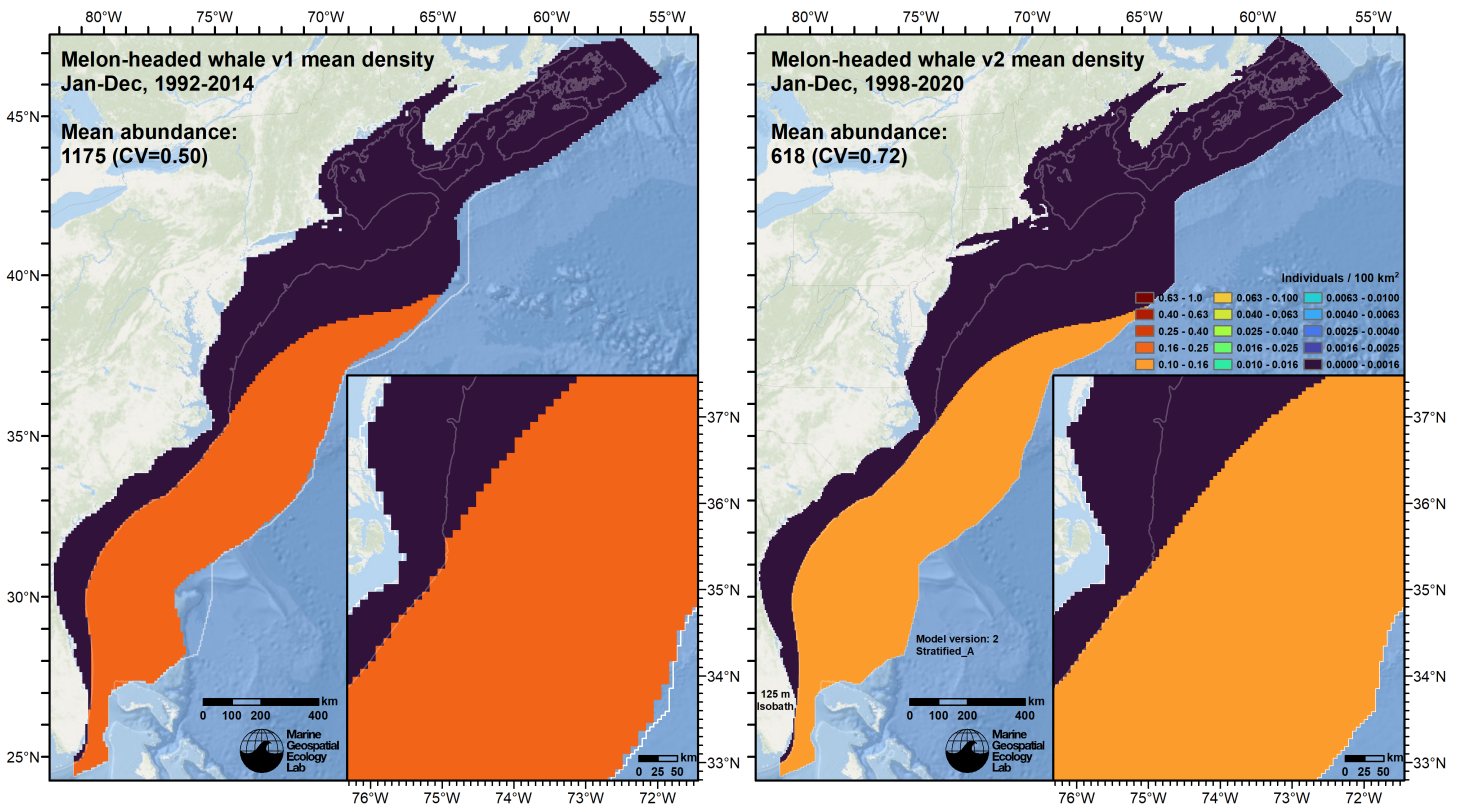


Figure 35: Comparison of the mean density predictions from the previous model (left) released by Roberts et al. (2016) to those from this model (right).

7 Discussion

Melon-headed whales are found in tropical and subtropical waters worldwide, and occasionally at higher latitudes often in association with incursions of warm water currents (Perryman and Danil 2018). In our east coast study area, the surveys contributed by the collaborators reported only four sightings, all in the Gulf Stream near Cape Hatteras, North Carolina,

consistent with the described habitat of higher latitudes that have incursions of warm water currents. In contrast, in the Gulf of Mexico, which is probably better habitat due to its consistently warm waters, the surveys contributed by SEFSC reported more than 25 sightings (Table 4).

The Gulf of Mexico surveys were not used directly in the east coast density estimate documented here, but were used indirectly, to fit a model for reclassifying ambiguous “Pygmy killer or melon-headed whale” sightings (Section 2). Six ambiguous sightings occurred in the east coast study area, all during SEFSC shipboard surveys (AMAPPS and pre-AMAPPS). All were classified as pygmy killer whales, on the basis of their small group sizes, which ranged from 2-8. We caution that if they were actually melon-headed whales, then this misclassification caused us to underestimate the density of melon-headed whales and overestimate the density of pygmy killer whales. However, because the mean group size (4.6) of the 6 ambiguous sightings was small relative to the mean group size (95) of the 3 definitive melon-headed whale sightings, the underestimation would be at most about 20%, once perception bias was accounted for.

With insufficient sightings to model density from environmental predictors, we estimated density in five geographic strata with a simplified approach (Section 5). The stratum over which we assumed melon-headed whales were present was similar to our prior model (Figure 35). Total abundance was 618 (Table 17), about 47% lower than our prior estimate of 1175 (Roberts et al. 2016). The estimates were within each other’s confidence limits. The main reason the new estimate is lower is that substantial effort was added (e.g. all of the NOAA AMAPPS program) without any new sightings. We also reformulated and refitted all detection functions, which resulted in one of the four sightings being truncated, which was not truncated in the prior analysis. However, this resulted from a reduction in the right-truncation distance for the detection function in question, which compensates for the loss of the sighting.

At the time of this writing, the NOAA Stock Assessment Reports had never listed an abundance estimate for melon-headed whale in the North Atlantic.

References

- Barco SG, Burt L, DePerte A, Digiovanni R Jr. (2015) Marine Mammal and Sea Turtle Sightings in the Vicinity of the Maryland Wind Energy Area July 2013-June 2015, VAQF Scientific Report #2015-06. Virginia Aquarium & Marine Science Center Foundation, Virginia Beach, VA
- Barlow J, Forney KA (2007) [Abundance and population density of cetaceans in the California Current ecosystem](#). Fishery Bulletin 105:509–526.
- Breiman L (2001) Random Forests. Machine Learning 45:5–32. doi: [10.1023/A:1010933404324](#)
- Buckland ST, Anderson DR, Burnham KP, Laake JL, Borchers DL, Thomas L (2001) Introduction to Distance Sampling: Estimating Abundance of Biological Populations. Oxford University Press, Oxford, UK
- Burt ML, Borchers DL, Jenkins KJ, Marques TA (2014) Using mark-recapture distance sampling methods on line transect surveys. Methods in Ecology and Evolution 5:1180–1191. doi: [10.1111/2041-210X.12294](#)
- Carretta JV, Lowry MS, Stinchcomb CE, Lynn MS, E. CR (2000) Distribution and abundance of marine mammals at San Clemente Island and surrounding offshore waters: Results from aerial and ground surveys in 1998 and 1999. NOAA Administrative Report LJ-00-02. NOAA National Marine Fisheries Service, Southwest Fisheries Center, La Jolla, CA
- Cole T, Gerrior P, Merrick RL (2007) [Methodologies of the NOAA National Marine Fisheries Service Aerial Survey Program for Right Whales \(*Eubalaena glacialis*\) in the Northeast U.S., 1998-2006](#). U.S. Department of Commerce, Woods Hole, MA
- Cotter MP (2019) Aerial Surveys for Protected Marine Species in the Norfolk Canyon Region: 2018–2019 Final Report. HDR, Inc., Virginia Beach, VA
- Foley HJ, Paxton CGM, McAlarney RJ, Pabst DA, Read AJ (2019) Occurrence, Distribution, and Density of Protected Species in the Jacksonville, Florida, Atlantic Fleet Training and Testing (AFTT) Study Area. Duke University Marine Lab, Beaufort, NC
- Garrison LP, Martinez A, Maze-Foley K (2010) [Habitat and abundance of cetaceans in Atlantic Ocean continental slope waters off the eastern USA](#). Journal of Cetacean Research and Management 11:267–277.
- Geo-Marine, Inc. (2010) [New Jersey Department of Environmental Protection Baseline Studies Final Report Volume III: Marine Mammal and Sea Turtle Studies](#). Geo-Marine, Inc., Plano, TX
- Hayes SA, Josephson E, Maze-Foley K, Rosel PE, Byrd B, Chavez-Rosales S, Cole TV, Garrison LP, Hatch J, Henry A, Horstman SC, Litz J, Lyssikatos MC, Mullin KD, Orphanides C, Pace RM, Palka DL, Powell J, Wenzel FW (2020)

- [US Atlantic and Gulf of Mexico Marine Mammal Stock Assessments - 2019](#). NOAA National Marine Fisheries Service, Northeast Fisheries Science Center, Woods Hole, MA
- Hothorn T, Hornik K, Zeileis A (2006) Unbiased Recursive Partitioning: A Conditional Inference Framework. *Journal of Computational and Graphical Statistics* 15:651–674. doi: [10.1198/106186006X133933](#)
- Laake JL, Calambokidis J, Osmek SD, Rugh DJ (1997) Probability of Detecting Harbor Porpoise From Aerial Surveys: Estimating $g(0)$. *Journal of Wildlife Management* 61:63–75. doi: [10.2307/3802415](#)
- Leiter S, Stone K, Thompson J, Accardo C, Wikgren B, Zani M, Cole T, Kenney R, Mayo C, Kraus S (2017) North Atlantic right whale *Eubalaena glacialis* occurrence in offshore wind energy areas near Massachusetts and Rhode Island, USA. *Endang Species Res* 34:45–59. doi: [10.3354/esr00827](#)
- Mallette SD, Lockhart GG, McAlarney RJ, Cummings EW, McLellan WA, Pabst DA, Barco SG (2014) Documenting Whale Migration off Virginia's Coast for Use in Marine Spatial Planning: Aerial and Vessel Surveys in the Proximity of the Virginia Wind Energy Area (VA WEA), VAQF Scientific Report 2014-08. Virginia Aquarium & Marine Science Center Foundation, Virginia Beach, VA
- Mallette SD, Lockhart GG, McAlarney RJ, Cummings EW, McLellan WA, Pabst DA, Barco SG (2015) Documenting Whale Migration off Virginia's Coast for Use in Marine Spatial Planning: Aerial Surveys in the Proximity of the Virginia Wind Energy Area (VA WEA) Survey/Reporting Period: May 2014 - December 2014, VAQF Scientific Report 2015-02. Virginia Aquarium & Marine Science Center Foundation, Virginia Beach, VA
- Mallette SD, McAlarney RJ, Lockhart GG, Cummings EW, Pabst DA, McLellan WA, Barco SG (2017) [Aerial Survey Baseline Monitoring in the Continental Shelf Region of the VACAPES OPAREA: 2016 Annual Progress Report](#). Virginia Aquarium & Marine Science Center Foundation, Virginia Beach, VA
- Marsh H, Sinclair DF (1989) Correcting for Visibility Bias in Strip Transect Aerial Surveys of Aquatic Fauna. *The Journal of Wildlife Management* 53:1017. doi: [10.2307/3809604](#)
- McAlarney R, Cummings E, McLellan W, Pabst A (2018) Aerial Surveys for Protected Marine Species in the Norfolk Canyon Region: 2017 Annual Progress Report. University of North Carolina Wilmington, Wilmington, NC
- McLellan WA, McAlarney RJ, Cummings EW, Read AJ, Paxton CGM, Bell JT, Pabst DA (2018) Distribution and abundance of beaked whales (Family Ziphiidae) Off Cape Hatteras, North Carolina, U.S.A. *Marine Mammal Science*. doi: [10.1111/mms.12500](#)
- Mullin KD, Fulling GL (2003) [Abundance of cetaceans in the southern U.S. North Atlantic Ocean during summer 1998](#). *Fishery Bulletin* 101:603–613.
- O'Brien O, Pendleton DE, Ganley LC, McKenna KR, Kenney RD, Quintana-Rizzo E, Mayo CA, Kraus SD, Redfern JV (2022) Repatriation of a historical North Atlantic right whale habitat during an era of rapid climate change. *Sci Rep* 12:12407. doi: [10.1038/s41598-022-16200-8](#)
- Palka D, Aichinger Dias L, Broughton E, Chavez-Rosales S, Cholewiak D, Davis G, DeAngelis A, Garrison L, Haas H, Hatch J, Hyde K, Jech M, Josephson E, Mueller-Brennan L, Orphanides C, Pegg N, Sasso C, Sigourney D, Soldevilla M, Walsh H (2021) [Atlantic Marine Assessment Program for Protected Species: FY15 – FY19 \(OCS Study BOEM 2021-051\)](#). U.S. Department of the Interior, Bureau of Ocean Energy Management, Washington, DC
- Palka DL (2006) [Summer abundance estimates of cetaceans in US North Atlantic navy operating areas \(NEFSC Reference Document 06-03\)](#). U.S. Department of Commerce, Northeast Fisheries Science Center, Woods Hole, MA
- Palka DL, Chavez-Rosales S, Josephson E, Cholewiak D, Haas HL, Garrison L, Jones M, Sigourney D, Waring G, Jech M, Broughton E, Soldevilla M, Davis G, DeAngelis A, Sasso CR, Winton MV, Smolowitz RJ, Fay G, LaBrecque E, Leiness JB, Dettloff K, Warden M, Murray K, Orphanides C (2017) [Atlantic Marine Assessment Program for Protected Species: 2010-2014 \(OCS Study BOEM 2017-071\)](#). U.S. Department of the Interior, Bureau of Ocean Energy Management, Washington, DC
- Perkins NJ, Schisterman EF (2006) The Inconsistency of "Optimal" Cutpoints Obtained using Two Criteria based on the Receiver Operating Characteristic Curve. *American Journal of Epidemiology* 670–675.
- Perryman WL, Danil K (2018) [Melon-Headed Whale](#). In: *Encyclopedia of Marine Mammals*. Elsevier, pp 593–595
- Quintana-Rizzo E, Leiter S, Cole T, Hagbloom M, Knowlton A, Nagelkirk P, O'Brien O, Khan C, Henry A, Duley P, Crowe L, Mayo C, Kraus S (2021) Residency, demographics, and movement patterns of North Atlantic right whales *Eubalaena glacialis* in an offshore wind energy development area in southern New England, USA. *Endang Species Res* 45:251–268. doi: [10.3354/esr01137](#)
- Read AJ, Barco S, Bell J, Borchers DL, Burt ML, Cummings EW, Dunn J, Fougères EM, Hazen L, Hodge LEW, Laura A-M, McAlarney RJ, Peter N, Pabst DA, Paxton CGM, Schneider SZ, Urian KW, Waples DM, McLellan WA (2014)

- Occurrence, distribution and abundance of cetaceans in Onslow Bay, North Carolina, USA. *Journal of Cetacean Research and Management* 14:23–35.
- Redfern JV, Kryc KA, Weiss L, Hodge BC, O'Brien O, Kraus SD, Quintana-Rizzo E, Auster PJ (2021) Opening a Marine Monument to Commercial Fishing Compromises Species Protections. *Front Mar Sci* 8:645314. doi: [10.3389/fmars.2021.645314](https://doi.org/10.3389/fmars.2021.645314)
- Roberts JJ, Best BD, Mannocci L, Fujioka E, Halpin PN, Palka DL, Garrison LP, Mullin KD, Cole TVN, Khan CB, McLellan WA, Pabst DA, Lockhart GG (2016) Habitat-based cetacean density models for the U.S. Atlantic and Gulf of Mexico. *Scientific Reports* 6:22615. doi: [10.1038/srep22615](https://doi.org/10.1038/srep22615)
- Roberts JJ, Yack TM, Halpin PN (2023) Marine mammal density models for the U.S. Navy Atlantic Fleet Training and Testing (AFTT) study area for the Phase IV Navy Marine Species Density Database (NMSDD), Document Version 1.3. Duke University Marine Geospatial Ecology Lab, Durham, NC
- Ryan C, Boisseau O, Cucknell A, Romagosa M, Moscrop A, McLanaghan R (2013) [Final report for trans-Atlantic research passages between the UK and USA via the Azores and Iceland, conducted from R/V Song of the Whale 26 March to 28 September 2012](#). Marine Conservation Research International, Essex, UK
- Schick R, Halpin P, Read A, Urban D, Best B, Good C, Roberts J, LaBrecque E, Dunn C, Garrison L, Hyrenbach K, McLellan W, Pabst D, Palka D, Stevick P (2011) Community structure in pelagic marine mammals at large spatial scales. *Marine Ecology Progress Series* 434:165–181. doi: [10.3354/meps09183](https://doi.org/10.3354/meps09183)
- Stone KM, Leiter SM, Kenney RD, Wikgren BC, Thompson JL, Taylor JKD, Kraus SD (2017) Distribution and abundance of cetaceans in a wind energy development area offshore of Massachusetts and Rhode Island. *J Coast Conserv* 21:527–543. doi: [10.1007/s11852-017-0526-4](https://doi.org/10.1007/s11852-017-0526-4)
- West KL, Walker WA, Baird RW, Webster DL, Schorr GS (2018) Stomach contents and diel diving behavior of melon-headed whales (*Peponocephala Electra*) in Hawaiian waters. *Mar Mam Sci* 34:1082–1096. doi: [10.1111/mms.12507](https://doi.org/10.1111/mms.12507)
- Whitt AD, Powell JA, Richardson AG, Bosyk JR (2015) [Abundance and distribution of marine mammals in nearshore waters off New Jersey, USA](#). *Journal of Cetacean Research and Management* 15:45–59.